Journal of Sound and Vibration (1997) **207**(2), 175–205

FREE SURFACE EFFECTS ON THE DYNAMICS OF CYLINDRICAL SHELLS PARTIALLY FILLED WITH LIQUID

A. A. Lakis and S. Neagu

Department of Mechanical Engineering, Applied Mechanics Section, École Polytechnique de Montréal, C.P. 6079, *succ. Centre-ville, Montréal, Québec, H3C* 3*A*7, *Canada*

(*Received* 22 *July* 1996, *and in final form* 4 *April* 1997)

This paper presents an analytical model for the dynamic analysis of thin cylindrical shells partially filled with liquid. The method used is a combination of finite element analysis and classical shell theory, and the objective is to determine the specific displacement functions which best represent the real deformations. The effect of oscillations of the free surface of the liquid on fluid-shell vibration is studied, and consideration is given to the influence of such parameters as: the circumferential mode, the axial mode, the structural damping, the length of the shell and the forces induced by the liquid. The shell is divided into cylindrical finite elements and the displacement functions are derived using Sander's thin shell theory. The stiffness and mass matrices of the shell are derived analytically. For the liquid contained in the shell, boundary conditions are prescribed and the behaviour of the liquid is expressed by a potential function. The kinetic and potential energies of the liquid are evaluated in order to establish the influence of surface oscillation on fluid-shell vibration.

1. INTRODUCTION

As thin shells are used in a variety of applications, they continue to arouse the interest of researchers who study their behaviour under dynamic and static loads. Thin shells are commonly used in the aeronautical industry, in the generation of nuclear energy and in the construction industry. Cylindrical shapes are also widely used in various forms as pressurised containers, pipes, and structural components.

The presence of a liquid inside a shell has an important influence on the dynamic behaviour of the structure and can create problems which are difficult to solve. In the design of liquid-filled structures, the calculation of the natural frequencies of the system is a preliminary step in the dynamic analysis.

Numerous researchers have studied the hydrodynamic coupling between the liquid and the structure using three forces: inertial, Coriolis and centrifugal. The term inertial is used to designate the virtual mass added to the mass of the structure. Among the studies carried out in the field of fluid–shell interaction, one can isolate several principal phenomena: hydrodynamic coupling, free surface motion of the liquid or "sloshing", and vibrations occurring when the liquid is flowing.

In the case of shells partially filled with liquid, free surface motion may be coupled to shell motion [1]. The latter case is of importance in the propellant tanks of liquid-propelled

0022–460X/97/420175 + 31 $25.00/0/sv971074

rockets and has received considerable attention. Other effects of the coupled fluid–shell motion occur when the fluid is flowing. Depending on the boundary conditions, buckling and flutter instabilities are possible in the beam modes of the shell [2, 3], and also in the shell modes [4], at sufficiently high flow velocities.

The first studies—and those which constitute the basic theories for the behaviour of a liquid inside a cylindrical, spherical or other shell, date from the 19th century and can be found in the works of Rayleigh and Lamb [5]. After World War II, technological and scientific advances gave a new impetus to this field as programs were developed for research into space flight.

Prominent among the studies of the 1960s was that of Berry and Reissner [6], who studied the behaviour of a pressurised liquid inside a cylindrical shell. The two researchers employed thin shell theory for cylindrical shells to investigate the static internal pressure load, the inertia of the shell due to radial movement and the inertia of the liquid due to the mass of the pressurised liquid. Lindholm *et al*. [1] analysed the vibrations of thin shells partially filled with liquid in the case of unpressurised cylindrical shells. It is necessary to consider also the work of Coale and Nagano [7], who studied the case of a cylindrical shell joined to a spherical shell, both filled with liquid.

More recently, Lakis *et al*. [8–12] studied the effects of the pressure and flow of internal or external liquid on the dynamics of thin shells. Bauer [13] studied the effects of an elastic surface cover on the vibrations of a rigid shell partially filled with liquid. Yamaki *et al*. [14] and Mazúch *et al*. [15] investigated the dynamic of cylindrical shell partially filled with liquid in the cases of clamped–clamped and clamped–free shells, respectively. On the other hand, Gonçalves and Ramos [16] developed a model for evaluating the free vibration of circular cylindrical shells partially filled with liquid by solving Sanders' shell equation using the Galerkin error minimization procedure.

2. THEORY

2.1. GENERAL APPROACH

In this paper the authors concentrate exclusively on the theoretical determination of the free vibration characteristics of thin, circular shells, partially or completely filled with liquid. The shell may be uniform or axially non-uniform. Only the so-called "breathing" modes of the shell will be considered ($n \geqslant 2$). It should be noted that the lowest frequencies are not generally associated with $n = 0$, axisymmetric, and $n = 1$, beam-like. Deformations in these modes involve more strain energy than some of those with $n \geqslant 2$. For more details, see Lakis and Sinno [17].

The finite element chosen is a cylindrical frustum, rather than the more usual triangular or rectangular flat plate elements. This allows us to use the shell equations in full for the determination of the displacement functions. For partially filled cylindrical shells, the shell is divided into its empty and full parts, and each is subdivided into a number of finite elements. The analysis for an empty finite element will be first presented and then modified for a fluid-filled element.

The displacement functions are determined by Sanders' theory for thin cylindrical shells [18, 19], rather than by, for example, Love's or Timoshenko's theories, for the following reason: in Sanders' theory all strains vanish for small rigid-body motion, which is not true for the other theories [20]; accordingly, the displacement functions based on Sanders' theory may be expected to satisfy the convergence criterion of the finite-element method stating that strains within the element should be zero when the nodal displacements are generated by rigid-body motion.

The dynamic behaviour of the system is governed by the equation of motion

$$([\mathbf{M}_0] - [\mathbf{M}_f]\{\ddot{\boldsymbol{\Delta}}\} - [\mathbf{C}_f]\{\dot{\boldsymbol{\Delta}}\} + ([\mathbf{K}_0] - [\mathbf{K}_f])\{\boldsymbol{\Delta}\} = \{\mathbf{F}(t)\}, \tag{1}$$

where $[\mathbf{M}_0]$ and $[\mathbf{K}_0]$ represent the mass and stiffness matrices of the solid shell (see Lakis and Paidoussis [10]), $[\mathbf{M}_f]$, $[\mathbf{C}_f]$ and $[\mathbf{K}_f]$ are the matrices associated with the inertia, Coriolis and centrifugal forces, respectively, and represent the effect of the liquid on the shell (see reference [11]). $\{\mathbf{F}(t)\}$ is the vector of the forces due to a random pressure field (see reference [12]); and $\boldsymbol{\Delta} = \{\boldsymbol{\delta}_1, \boldsymbol{\delta}_2, \ldots, \boldsymbol{\delta}_{N+1}\}^{\mathrm{T}}$ where $\boldsymbol{\delta}_{N+1}$ is the displacement vector associated with the second node of the last finite element. A list of symbols appears in Appendix B.

In the case of liquid at rest, the matrices $[\mathbf{C}_f]$, $[\mathbf{K}_f]$ and $\{\mathbf{F}(t)\}$ are null and equation (1) takes the form

$$([\mathbf{M}_0] - [\mathbf{M}_f])\{\ddot{\boldsymbol{\Delta}}\} + [\mathbf{K}_0]\{\boldsymbol{\Delta}\} = \{\mathbf{0}\}. \tag{2}$$

In equations (1) and (2), the effects induced by the free surface of the liquid have been ignored. In order to account for them, a mass matrix for the surface in movement and a stiffness matrix for the change in potential of the liquid due to the height of the waves will be added:

$$([\mathbf{M}_0] - ([\mathbf{M}_f] + [\mathbf{M}_{fs}]))\{\ddot{\boldsymbol{\Delta}}\} + ([\mathbf{K}_0] - [\mathbf{K}_{fs}])\{\boldsymbol{\Delta}\} = \{\mathbf{0}\}. \tag{3}$$

Finally, with the notations $[\mathbf{M}_F] = -[\mathbf{M}_f] - [\mathbf{M}_{fs}]$ and $[\mathbf{K}_F] = -[\mathbf{K}_{fs}]$ one finds the following equation of motion for the dynamic behaviour of the system:

$$([\mathbf{M}_0] + [\mathbf{M}_F])\{\ddot{\boldsymbol{\Delta}}\} + ([\mathbf{K}_0] + [\mathbf{K}_F])\{\boldsymbol{\Delta}\} = \{\mathbf{0}\}. \tag{4}$$

The matrices $[\mathbf{M}_0]$, $[\mathbf{K}_0]$ have previously been calculated by Lakis *et al*. [10]. In this study, therefore, matrices $[\mathbf{M}_F]$ and $[\mathbf{K}_F]$ are developed to model the behaviour of the liquid taking into account the free surface motion. Then, to analyse the effect of the surface oscillations, one compares the results obtained by this method with those obtained by Lakis and Paidoussis [11], who did not take the free surface effects into account.

In this work, the influence of various parameters, such as: the circumferential and axial modes, the structural damping, the length of the shell and the inertial forces induced by the liquid and its free surface is considered.

For a thin cylindrical shell specific displacement functions using shell theory are calculated. Using these results in conjunction with finite element analysis, one finds the mass and stiffness matrices of the solid shell and the equations of motion. Taking into account the impermeability conditions of the fluid-structure interface, the behaviour of the liquid element is expressed using a potential function. The kinetic and potential energies of the liquid mass are calculated in order to determine the effect of the liquid of the motion of the free surface on the fluid-shell vibrations.

2.2. DISPLACEMENT FUNCTIONS

A cylindrical finite element is used, which is bounded at its extremities by two circular nodes i and j (Figures 1, 2 and 3). The displacement functions can be expressed in a general form as

$$\begin{Bmatrix} U(x,\theta) \\ V(x,\theta) \\ W(x,\theta) \end{Bmatrix} = [\mathbf{N}] \begin{Bmatrix} \boldsymbol{\delta}_i \\ \boldsymbol{\delta}_j \end{Bmatrix}, \tag{5}$$

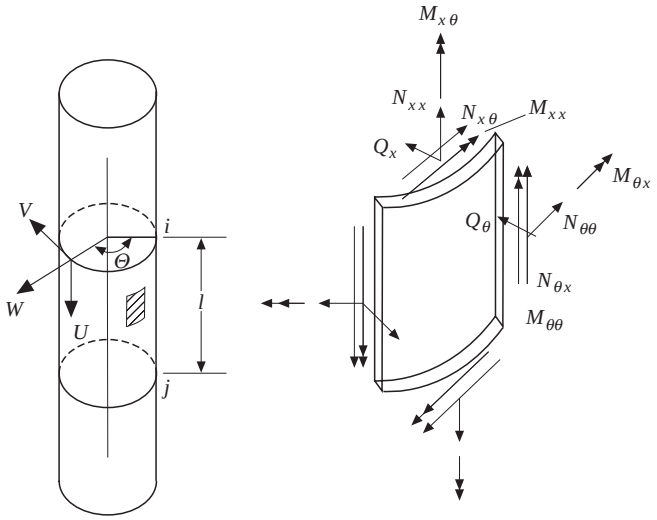

Figure 1. Cylindrical shell with differential element.

where the elements of matrix **[N]** are a function of the position and of the anisotropy of the shell, and where the vector $\{\boldsymbol{\delta}_i \boldsymbol{\delta}_j\}^{\mathrm{T}}$ represents the nodal displacements.

To study the equilibrium of the cylindrical shell while taking into account the effects of the membrane and also of the bending of the mean surface, Sanders' first order equations [21] are used. These equations are based on Love's first approximation and permit zero deformations in the case of small movements of the rigid body, which is not the case with other theories. The equilibrium equations for thin cylindrical shells are given in Appendix A.1.

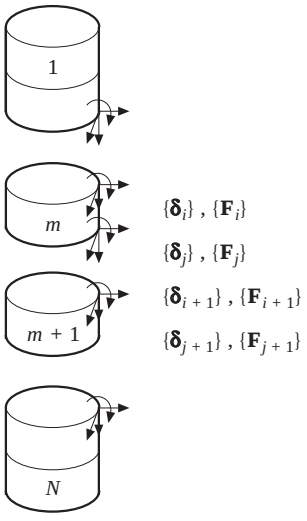

Figure 2. Division of the shell.

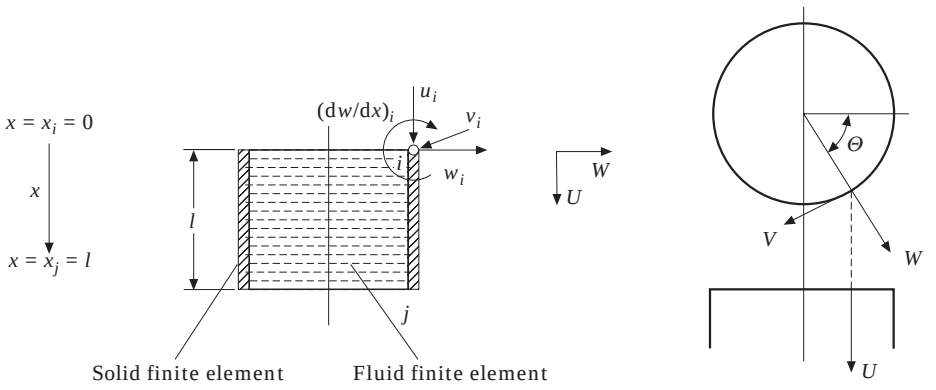

Figure 3. Displacements and degrees of freedom at a node.

The general shape of the displacement functions (in cylindrical co-ordinates in the axial, tangential and radial directions, taking account of their periodicity in the circumferential direction) is given by

$$U = \sum_n u_n(x) \cos n\theta, \qquad V = \sum_n v_n(x) \sin n\theta, \qquad W = \sum_n w_n(x) \cos n\theta, \tag{6}$$

where n is the number of circumferential modes, x is the co-ordinate along the axis of the cylinder, and θ is the co-ordinate in the circumferential direction. For the axial direction one assumes

$$u_n(x) = \mathrm{A}\, \mathrm{e}^{\lambda x/r}, \qquad v_n(x) = \mathbf{B}\, \mathrm{e}^{\lambda x/r}, \qquad w_n(x) = \mathbf{C}\, \mathrm{e}^{\lambda x/r}, \tag{7}$$

where r is the average shell radius and $\mathbf{A}$, $\mathbf{B}$, $\mathbf{C}$ and $\boldsymbol{\lambda}$ are complex numbers.

When the given displacement functions are replaced by equations (5) and (6) in the equilibrium equations (see Appendix A.1., equations (A.4–6), one obtains a three-equation linear system:

$$[\mathbf{H}] \begin{Bmatrix} \mathbf{A} \\ \mathbf{B} \\ \mathbf{C} \end{Bmatrix} = 0. \tag{8}$$

For the non-trivial solution, the determinant of matrix [**H**] must vanish, which gives one a characteristic eighth order equation in $\boldsymbol{\lambda}$:

$$h_8\boldsymbol{\lambda}^8 + h_6\boldsymbol{\lambda}^6 + h_4\boldsymbol{\lambda}^4 + h_2\boldsymbol{\lambda}^2 + h_0 = 0, \tag{9}$$

where the matrix [**H**] is given in Appendix A and the terms h_i ($i = 0$, 2, 4, 6 and 8) are given in reference [10]. The solution of equation (9) gives the values of $\boldsymbol{\lambda}_i$ ($i = 1$–8).

Each value of $\boldsymbol{\lambda}_i$ constitutes a solution of the equilibrium equations and the complete solution is a linear combination of those equations with constant $\mathbf{A}_j$, $\mathbf{B}_j$ and $\mathbf{C}_j$, where j varies from 1–8.

Since $\mathbf{A}_j$, $\mathbf{B}_j$ and $\mathbf{C}_j$ are not independent, one expresses $\mathbf{A}_j$ and $\mathbf{B}_j$ as a function of $\mathbf{C}_j$, using complex constants $\boldsymbol{\alpha}_j$ and $\boldsymbol{\beta}_j$:

$$\mathbf{A}_j = \boldsymbol{\alpha}_j \mathbf{C}_j, \qquad \mathbf{B}_j = \boldsymbol{\beta}_j \mathbf{C}_j. \tag{10}$$

The final shape of the matrix can therefore be written as follows (for more details, see Lakis and Paidoussis [10]):

$$\begin{Bmatrix} \mathbf{U} \\ \mathbf{V} \\ \mathbf{W} \end{Bmatrix} = [\mathbf{T}][\mathbf{R}]\{\mathbf{C}\}, \tag{11}$$

where [**T**] and [**R**] are (3 × 3) and (3 × 8) matrices and are given in Appendix A. The vector $\{\mathbf{C}\}$ contains the only free constants of the problem, which are expressed as a function of the nodal displacements of the elements,

$$\{\mathbf{C}\} = \begin{Bmatrix} \bar{\mathbf{C}}_1 \\ \bar{\mathbf{C}}_2 \\ \vdots \\ \bar{\mathbf{C}}_8 \end{Bmatrix}. \tag{12}$$

The displacements of node i are defined by the vector

$$\{\boldsymbol{\delta}_i\} = \begin{Bmatrix} u_{ni} \\ w_{ni} \\ (\mathrm{d}w_n/\mathrm{d}x)_i \\ v_{ni} \end{Bmatrix}. \tag{13}$$

All the components of vector $\{\boldsymbol{\delta}_i\}$ represent the magnitude of the displacements U, W, $\mathrm{d}W/\mathrm{d}x$ and V associated with the circumferential mode n. Each element has two nodes and eight degrees of freedom (see also Figure 3):

$$\begin{Bmatrix} \boldsymbol{\delta}_i \\ \boldsymbol{\delta}_j \end{Bmatrix} = \begin{Bmatrix} u_{ni} \\ w_{ni} \\ (\mathrm{d}w_n/\mathrm{d}x)_i \\ v_{ni} \\ u_{nj} \\ w_{nj} \\ (\mathrm{d}w_n/\mathrm{d}x)_j \\ v_{nj} \end{Bmatrix} = [\mathbf{A}]\{\mathbf{C}\}. \tag{14}$$

The terms of matrix [**A**] are obtained from the values of matrix [**R**] and are given in Appendix A.

By multiplying by $[\mathbf{A}]^{-1}$ one obtains the matrix for the constant $\mathbf{C}_j$ as a function of the degrees of freedom:

$$\{\mathbf{C}\} = [\mathbf{A}]^{-1}\begin{Bmatrix} \boldsymbol{\delta}_i \\ \boldsymbol{\delta}_j \end{Bmatrix}. \tag{15}$$

Finally, one substitutes the vector $\{\mathbf{C}\}$ into equation (11) and obtains the displacement functions as follows:

$$\begin{Bmatrix} U \\ V \\ W \end{Bmatrix} = [\mathbf{T}][\mathbf{R}][\mathbf{A}]^{-1}\begin{Bmatrix} \boldsymbol{\delta}_i \\ \boldsymbol{\delta}_j \end{Bmatrix} = [\mathbf{N}]\begin{Bmatrix} \boldsymbol{\delta}_i \\ \boldsymbol{\delta}_j \end{Bmatrix}. \tag{16}$$

Matrices [**T**], [**R**] and [**A**] are given in Appendix A.

2.3. MASS AND STIFFNESS MATRICES FOR AN EMPTY SHELL

The strain vector $\{\epsilon\}$ can be determined from the displacement functions U, V, W and the deformation–displacement equations presented in Appendix A as

$$\{\boldsymbol{\epsilon}\} = \begin{Bmatrix} \epsilon_x \\ \epsilon_\theta \\ 2\bar{\epsilon}_{x\theta} \\ k_x \\ k_\theta \\ 2\bar{k}_{x\theta} \end{Bmatrix} = \begin{bmatrix} [\mathbf{T}][\mathbf{0}] \\ [\mathbf{0}][\mathbf{T}] \end{bmatrix} [\mathbf{Q}][\mathbf{A}]^{-1} \begin{Bmatrix} \boldsymbol{\delta}_i \\ \boldsymbol{\delta}_j \end{Bmatrix} = [\mathbf{B}] \begin{Bmatrix} \boldsymbol{\delta}_i \\ \boldsymbol{\delta}_j \end{Bmatrix}, \tag{17}$$

where matrices [**T**] and [**Q**] are also given in Appendix A.

The stress vector $\{\boldsymbol{\sigma}\}$ may be expressed as a function of the strain, $\{\boldsymbol{\epsilon}\}$, as

$$\{\boldsymbol{\sigma}\} = \begin{Bmatrix} N_x \\ N_\theta \\ \bar{N}_{x\theta} \\ M_x \\ M_\theta \\ \bar{M}_{x\theta} \end{Bmatrix} = [\mathbf{P}]\{\boldsymbol{\epsilon}\} = [\mathbf{P}][\mathbf{B}] \begin{Bmatrix} \boldsymbol{\delta}_i \\ \boldsymbol{\delta}_j \end{Bmatrix}. \tag{18}$$

For an isotropic cylindrical shell the elasticity matrix [**P**] takes the form

$$[\mathbf{P}] = \begin{bmatrix} D & vD & 0 & 0 & 0 & 0 \\ vD & D & 0 & 0 & 0 & 0 \\ 0 & 0 & (1-v)D/2 & 0 & 0 & 0 \\ 0 & 0 & 0 & K & vK & 0 \\ 0 & 0 & 0 & vK & K & 0 \\ 0 & 0 & 0 & 0 & 0 & (1-v)K/2 \end{bmatrix}, \tag{19}$$

with the parameters D = membrane stiffness, K = bending stiffness:

$$K = Et^3/12(1-v^2), \qquad D = Et/(1-v^2). \tag{20}$$

For the most general case, that of an orthotropic cylindrical shell, the matrix [**P**] is more complex and may be written as

$$[\mathbf{P}] = \begin{bmatrix} P_{11} & P_{12} & 0 & P_{14} & P_{15} & 0 \\ P_{21} & P_{22} & 0 & P_{24} & P_{25} & 0 \\ 0 & 0 & P_{33} & 0 & 0 & P_{36} \\ P_{41} & P_{42} & 0 & P_{44} & P_{45} & 0 \\ P_{51} & P_{52} & 0 & P_{54} & P_{55} & 0 \\ 0 & 0 & P_{63} & 0 & 0 & P_{66} \end{bmatrix}. \tag{21}$$

Coefficients P_{ij} are given in reference [22].

The mass and stiffness matrices are then expressed as a function of equations (17) to (21):

$$[\mathbf{k}_0] = \iint_A [\mathbf{B}]^T[\mathbf{P}][\mathbf{B}]\,\mathrm{d}A, \qquad [\mathbf{m}_0] = \rho t \iint_A [\mathbf{N}]^T[\mathbf{N}]\,\mathrm{d}A, \tag{22, 23}$$

where ρ is the density and t is the thickness of the shell.

The surface element of the shell wall is $dA = r\,\mathrm{d}\theta\,\mathrm{d}x$. After integrating over θ, the preceding equations become

$$[\mathbf{k}_0] = \pi r[\mathbf{A}^{-1}]^T\left(\int_0^1 [\mathbf{Q}]^T[\mathbf{P}][\mathbf{Q}]\,\mathrm{d}x\right)[\mathbf{A}^{-1}], \qquad [\mathbf{m}_0] = \pi r\rho t[\mathbf{A}^{-1}]^T\left(\int_0^1 [\mathbf{R}]^T[\mathbf{R}]\,\mathrm{d}x\right)[\mathbf{A}^{-1}]. \tag{24}$$

$[\mathbf{k}_0]$ and $[\mathbf{m}_0]$ were obtained analytically by carrying out the necessary matrix operations and integrations over x in equation (24). To do this it was found necessary to introduce several intermediate matrices, eventually obtaining expressions for the general terms k_{pc} and m_{pq} of $[\mathbf{k}_0]$ and $[\mathbf{m}_0]$, respectively. Because of the complexity of the manipulations, neither the intermediate steps nor the final result will be given here. See references [10] or [23] for details.

From these equations, one can assemble the mass and stiffness matrices for each element to obtain the mass and stiffness matrices for the whole shell: $[\mathbf{M}_0]$ and $[\mathbf{K}_0]$. Each elementary matrix is (8×8), therefore the final dimensions of $[\mathbf{M}_0]$ and $[\mathbf{K}_0]$ will be $4(N + 1)$, where N is the number of elements of the shell.

2.4. ANALYSIS FOR A FLUID-FILLED SHELL

The authors consider that the dynamic behaviour of a cylindrical shell under pressure from internal fluid is governed by the equation of motion (4). In order to analyse the behaviour of the fluid inside the shell, a mathematical model has been developed based on the following hypotheses: the fluid is incompressible; the motion of the fluid is irrotational and inviscid; the energy of the fluid will be derived from the potential flow theory; only small vibrations (linear theory) will be considered and the pressure of the fluid inside the shell is taken to be purely radial.

Suppose one has a cylindrical fluid finite element with two nodes i and j; and for each node the displacements are given by the vector (see Figures 3 and 4):

$$\{\boldsymbol{\delta}_i\} = \begin{Bmatrix} u_{ni} \\ w_{ni} \\ (\mathrm{d}w_n/\mathrm{d}x)_i \\ v_{ni} \end{Bmatrix}, \tag{25}$$

where u_{ni}, v_{ni} and w_{ni} are the components of the axial, radial and tangential displacements associated with the circumferential mode n.

The equations which govern the irrotational motion of the liquid cylinder can be expressed as a function of velocity potential ϕ. The velocity components are given by derivatives of the potential function. Using cylindrical co-ordinates, one has the equations

$$V_x = \partial\phi/\partial x, \qquad V_r = \partial\phi/\partial r, \qquad V_\theta = \partial\phi/r\,\partial\theta, \tag{26}$$

where x, θ and r are the co-ordinates in the axial, circumferential and radial directions of the cylinder.

For an incompressible fluid (ρ = constant) and irrotational flow, the motion is governed by the continuity equation:

$$(1/r)\,\partial/\partial r(r\,\partial\phi/\partial r) + (1/r^2)\,\partial^2\phi/\partial\theta^2 + \partial^2\phi/\partial x^2 = 0. \tag{27}$$

The associated boundary conditions are

$$\partial\phi/\partial r|_{r=0} = 0, \tag{28}$$

which ensures a finite solution on the axis at $r = 0$;

$$p = \text{const}|_{x=h} \tag{29}$$

on the free surface of the fluid; and

$$v_r|_{r=a} = \partial w/\partial t. \tag{30}$$

At the solid boundary the velocity of the fluid is equal to that of the wall (in the case of an undisturbed fluid); a is the internal radius and here t indicates time.

2.5. INFLUENCE OF THE FREE SURFACE OF THE FLUID

To determine the influence of the free surface, one applies Bernoulli's equation in its general form:

$$p/\rho = -\partial\phi/\partial t + \mathrm{g}x + f(t), \tag{31}$$

where $f(t)$ is a function that varies with time t, and which will be included in the value of $\partial\phi/\partial t$, g is the acceleration of gravity and x is the height of the fluid required to calculate the pressure (see Figure 4).

Let η be the height of one point on the surface at a given time t with reference to the flat horizontal surface (see Figure 4). Since the pressure (p) is either constant or null at the surface, Bernoulli's equation (31) gives the value of η as

$$\eta = (1/\mathrm{g})[\partial\phi/\partial t]_{x=0}, \tag{32}$$

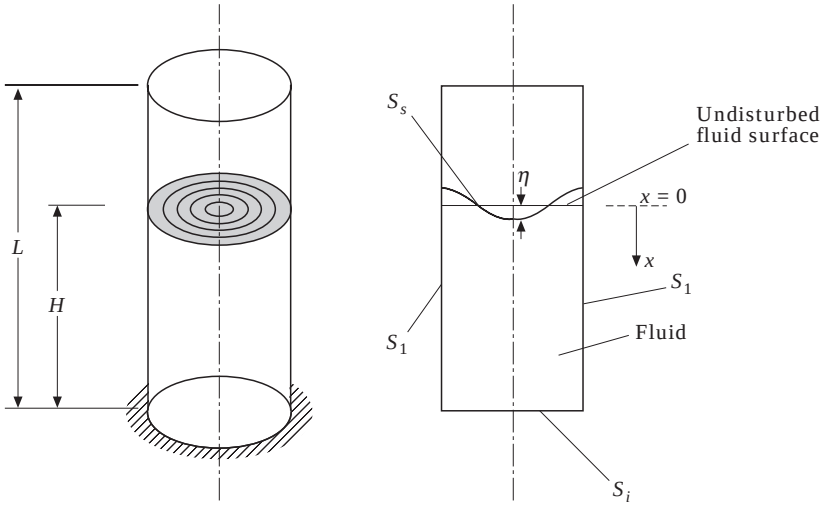

Figure 4. Cylindrical shell partially filled with fluid.

where η is calculated at $x = 0$ (see Figure 4), which is the height of the undisturbed surface.

Therefore, one obtains

$$[\partial^2\phi/\partial t^2 + g\,\partial\phi/\partial x]_{x=0} = 0. \tag{33}$$

Equation (33) gives the general linear condition associated with the free surface of the fluid.

To evaluate the influence of the surface motion on the fluid–shell vibrations, it is necessary to develop kinetic and potential energies during vibration. This approach, which was proposed by Lamb [5], leads us to an evaluation of the equations

$$T = \frac{\rho_F}{2} \iint_{S_s} \phi \frac{\partial\phi}{\partial n_s}\,\mathrm{d}s, \qquad V = \rho_F g \iiint_V x\,\mathrm{d}v, \tag{34, 35}$$

where S_s represents the upper or free surface of the fluid, n_s represents the normal to the free surface, positive outward and x represents the co-ordinate in the axial direction of the cylinder.

For potential energy, integration in the axial direction is done between 0 and η; 0 represents the fluid at rest and η is the height of the wave (see Figure 4).

The total kinetic energy of the fluid inside the shell may be written as

$$T = \frac{\rho_F}{2} \iiint_V [v_x^2 + v_r^2 + v_\theta^2]\,\mathrm{d}v. \tag{36}$$

By applying the Green–Gauss theorem to the volume integral of the kinetic energy, one obtains

$$\frac{2T}{\rho_F} = \iiint_V \left[\left(\frac{\partial\phi}{\partial x}\right)^2 + \left(\frac{\partial\phi}{\partial r}\right)^2 + \left(\frac{\partial\phi}{r\,\partial\theta}\right)^2\right]\mathrm{d}V = \iint_S \left[\phi\frac{\partial\phi}{\partial n}\right]\mathrm{d}S - \iiint_V [\phi\nabla^2\phi]\,\mathrm{d}V, \tag{37}$$

where S is the surface which surrounds the volume of fluid and n is the normal to this surface, positive outward.

But the continuity equation requires that $\nabla^2\phi = 0$, which cancels the last term of equation (37), which can then be rewritten as

$$\frac{2T}{\rho_F} = \iint_S \left[\phi\frac{\partial\phi}{\partial n}\right]\mathrm{d}S = \iint_{S_s} \left[\phi\frac{\partial\phi}{\partial n_s}\right]\mathrm{d}S + \iint_{S_1} \left[\phi\frac{\partial\phi}{\partial n_1}\right]\mathrm{d}S - \iint_{S_i} \left[\phi\frac{\partial\phi}{\partial n_i}\right]\mathrm{d}S, \tag{38}$$

where S_s and n_s are, respectively, the free surface (upper surface) and the normal to this surface, positive outward (see Figure 4), S_1 and n_1 represent, respectively, the lateral surface which surrounds the volume of fluid and the normal to this surface, positive outward and S_i and n_i indicate, respectively, the lower surface (at the base) and the normal to this surface, positive outward.

The first integral on S_s gives us the effect of the free surface motion. The second on the lateral surface (S_1) takes into account the effect of the dynamic pressure of the fluid at the boundary. The third integral is zero when the lower surface is identical to that of the rigid base of the solid cylinder because $\partial\phi/\partial n_i = 0$ (the velocity of the surface is zero in the latter case—see Figure 4). As far as the middle elements are concerned, the kinetic energy on the lower surface of the upper element is cancelled out by the kinetic energy on the upper surface of the lower element when one adds the energies of all the elements.

Therefore, one can calculate the influence of the fluid on the shell (taking into account the effects of the free surface as shown in equation (38)). This equation takes into account the energies of both the free surface and the lateral surface of the fluid.

2.6. SOLVING THE CONTINUITY EQUATION

The solution of the continuity equation has been developed in the work cited in references [11] and [22]. Here the case of zero velocity will be considered.

The radial displacement of the solid boundary, w, expressed by equation (16), may be rewritten as

$$w = \sum_{j=1}^{8} e^{i(\lambda_j x/a + \omega t)} \cos n\theta = \sum_{j=1}^{8} w_j \tag{39}$$

and the potential function $\phi = \phi(x, r, \theta, t)$ may be assumed as

$$\phi(x, r, \theta, t) = R(r)S(x, \theta, t). \tag{40}$$

Using equation (39), $\phi(x, r, \theta, t)$ can be expressed as the sum of eight components:

$$\phi(x, r, \theta, t) = \sum_{j=1}^{8} R_j(r)S_j(x, \theta, t). \tag{41}$$

By substituting equations (41) into the boundary condition of the shell wall given by equation (30) and using equation (39), one obtains

$$\phi(x, r, \theta, t) = \sum_{j=1}^{8} \frac{R_j(r)}{R_j'(a)} \dot{w}_j. \tag{42}$$

By introducing the velocity potential into the continuity equation (27), one may write

$$\sum_{j=1}^{8} \left\{ \frac{R_j''(r)}{R_j'(a)} \dot{w}_{nj} + \frac{R_j'(r)}{R_j'(a)} \dot{w}_{nj} - \frac{n^2}{r^2} \frac{R_j(r)}{R_j'(a)} [\dot{w}_{nj} + \dot{w}_{nj}''] \right\} \cos n\theta = 0. \tag{43}$$

The unknown function which remains to be determined is given by the radial variation of $R(r)$. This Bessel differential equation (43) presents a general solution of the form

$$R_j(r) = \mathbf{A}J_n(im_j r) + \mathbf{B}Y_n(im_j r), \tag{44}$$

where $J_n(im_j r)$ is the Bessel function of the first kind of order n, $Y_n(im_j r)$ is the Bessel function of the second kind of order n, $\mathbf{A}$ and $\mathbf{B}$ are constants to be determined and $m_j = \boldsymbol{\lambda}_j/a$ and $\boldsymbol{\lambda}_j$ with $j = 1, 2, \ldots, 8$ are the roots of the characteristic equation (9).

For internal flow at the centre of the cylinder at $r = 0$, the solution should be finite, but $\lim_{r\to 0} Y_n(im_j r) \to -\infty$; it is necessary therefore that $\mathbf{B} \to 0$. Thus one arrives at the solution to the differential equation (43):

$$R_j(r) = \mathbf{A}J_n(im_j r). \tag{45}$$

This last equation determines the variation of ϕ in the radial direction and gives the analytical form of the potential function

$$\phi(x, r, \theta, t) = \sum_{j=1}^{8} \frac{J_n(im_j r)}{J_n'(im_j a)} \dot{w}_j. \tag{46}$$

The general matrix shape of the radial displacement of the solid wall is known to be (see equation (11))

$$w = \cos n\theta \{\mathbf{R}_F\}^T \{\mathbf{C}\}, \tag{47}$$

where the vector of the constants $\{\mathbf{C}\}$ is defined by the equation

$$\begin{Bmatrix} \boldsymbol{\delta}_i \\ \boldsymbol{\delta}_j \end{Bmatrix} = [\mathbf{A}]\{\mathbf{C}\}, \tag{48}$$

and the terms of matrix [**A**] are obtained using the value of matrix [**R**] and are given in Appendix A; the vector $\{\mathbf{R}_F\}^T$ is the second line of matrix [**R**] which therefore corresponds to the radial displacement

$$\{\mathbf{R}_F\}^T = \{e^{i\lambda_1 x/a}\ e^{i\lambda_2 x/a}\ e^{i\lambda_3 x/a} \cdots e^{i\lambda_8 x/a}\}^T. \tag{49}$$

The matrix for the potential function (46) becomes

$$\phi(x, r, \theta, t) = \cos(n\theta)\{\mathbf{R}_F\}^T[\mathbf{H}_F][\mathbf{A}^{-1}]\{\dot{\mathbf{q}}\}, \tag{50}$$

where

$$\{\mathbf{q}\} = \begin{Bmatrix} \boldsymbol{\delta}_i \\ \boldsymbol{\delta}_j \end{Bmatrix} \tag{51}$$

and

$$H_F(j, k) = \begin{cases} \dfrac{J_n(im_j r)}{im_j J_n'(im_j a)}, & \text{for } j = k \text{ and } im_j = \dfrac{i\lambda_j}{a}, \quad i^2 = -1, \\ 0, & \text{for } j \neq k. \end{cases} \tag{52}$$

The potential function determined by equation (50) is dependent on the displacement vector $\{\mathbf{q}\}$ defined for each element. Therefore, as the solid shell is divided into several finite elements, the fluid is also divided into fluid finite elements, corresponding in each case to the solid element which surrounds it.

2.7. EVALUATION OF THE KINETIC ENERGY OF THE FLUID ELEMENT

To determine the equations of fluid motion, one evaluates the kinetic energy in order to find the corresponding mass matrix. The kinetic energy expressed in cylindrical co-ordinates is given by equation (37).

In order to make these calculations, one assumes the kinetic energy to be the sum of the components in three directions: axial, radial and circumferential,

$$T_e = T_x + T_R + T_\theta. \tag{53}$$

The derivative of the potential function is given by equation (50) in terms of x permits one to express the kinetic energy T_x as

$$T_x = \frac{\pi\rho_F}{2}\{\dot{\mathbf{q}}\}^T[\mathbf{A}^{-1}]^T \int_0^a [\mathbf{H}_x]^T \left(\int_0^1 \{\mathbf{R}_F\}\{\mathbf{R}_F\}^T \, dx \right) [\mathbf{H}_x] r \, dr [\mathbf{A}^{-1}]\{\dot{\mathbf{q}}\}, \tag{54}$$

where the terms of vector $\{\mathbf{R}_F\}$ and matrix $[\mathbf{A}]$ are given, respectively, by equations (48) and (49). The terms of matrix $[\mathbf{H}_x]$ can be written in the form

$$H_x(j,k) = \begin{cases} \mathrm{J}_n(\mathrm{i}m_j r)/\mathrm{J}_n(\mathrm{i}\boldsymbol{\lambda}_j), & \text{for } j = k, \\ 0, & \text{for } j \neq k, \end{cases} \tag{55}$$

where $m_j = \boldsymbol{\lambda}_j/a$, $\boldsymbol{\lambda}_j$ are the roots of the characteristic equation given by equation (9), $\mathrm{i}^2 = -1$ and a is the internal radius of the shell.

After integration, one can write

$$T_x = \tfrac{1}{2}\{\dot{\mathbf{q}}\}^{\mathrm{T}}[\mathbf{m}_x]\{\dot{\mathbf{q}}\}, \tag{56}$$

where

$$[\mathbf{m}_x] = \pi\rho_F[\mathbf{A}^{-1}]^{\mathrm{T}}[\mathbf{hx}][\mathbf{A}^{-1}]. \tag{57}$$

The calculation of matrix $[\mathbf{hx}]$ is given in Appendix A.

The same steps are followed in calculating the kinetic energy in the radial and tangential directions, with the partial derivatives of the potential function in terms of the radius (r) and the circumferential co-ordinate (θ), respectively.

One obtains, for T_R,

$$T_R = \tfrac{1}{2}\{\dot{\mathbf{q}}\}^{\mathrm{T}}[\mathbf{m}_R]\{\dot{\mathbf{q}}\}, \tag{58}$$

where

$$[\mathbf{m}_R] = \pi\rho_F[\mathbf{A}^{-1}]^{\mathrm{T}}[\mathbf{hr}][\mathbf{A}^{-1}]. \tag{59}$$

The calculation of matrix $[\mathbf{hr}]$ is given in Appendix A.

Finally, for T_θ,

$$T_\theta = \tfrac{1}{2}\{\dot{\mathbf{q}}\}^{\mathrm{T}}[\mathbf{m}_\theta]\{\dot{\mathbf{q}}\}, \tag{60}$$

where

$$[\mathbf{m}_\theta] = \pi\rho_F[\mathbf{A}^{-1}]^{\mathrm{T}}[\mathbf{h\theta}][\mathbf{A}^{-1}], \tag{61}$$

and matrix $[\mathbf{h\theta}]$ is given in Appendix A.

The total kinetic energy of a fluid finite element is the sum of the three components which have just been calculated, thus

$$T_e = \tfrac{1}{2}\{\dot{\mathbf{q}}\}^{\mathrm{T}}[\mathbf{m}_x]\{\dot{\mathbf{q}}\} + \tfrac{1}{2}\{\dot{\mathbf{q}}\}^{\mathrm{T}}[\mathbf{m}_r]\{\dot{\mathbf{q}}\} + \tfrac{1}{2}\{\dot{\mathbf{q}}\}^{\mathrm{T}}[\mathbf{m}_\theta]\{\dot{\mathbf{q}}\},$$

$$[\mathbf{m}_F] = [\mathbf{m}_x] + [\mathbf{m}_r] + [\mathbf{m}_\theta], \tag{62}$$

or

$$T_e = \tfrac{1}{2}\{\dot{\mathbf{q}}\}^{\mathrm{T}}[\mathbf{m}_F]\{\dot{\mathbf{q}}\}, \tag{63}$$

where $[\mathbf{m}_F]$ is a symmetrical (8×8) matrix which takes into account the inertia of the fluid element and that of the free surface.

2.8. POTENTIAL ENERGY OF THE FREE SURFACE OF THE FLUID

The potential function ϕ, given by equation (50), is replaced by the general equation associated with the free surface (33), and becomes

$$[\mathbf{R}_F]_0[\mathbf{H}_F][\mathbf{A}^{-1}]\{\ddot{\mathbf{q}}\} + \mathrm{g}[\mathbf{R}_F]_0[\mathrm{i}m_j][\mathbf{H}_F][\mathbf{A}^{-1}]\{\mathbf{q}\} = 0. \tag{64}$$

The potential energy of the wave system, due to the height of the fluid in terms of the mean surface, is given by Lamb [5] in the following way:

$$V = \rho_F \mathrm{g} \int_0^a \int_0^{2\pi} \int_0^{\eta} x \, \mathrm{d}x r \, \mathrm{d}\theta \, \mathrm{d}r. \tag{65}$$

The integration in terms of x should be done between 0 and η (η being the height of the wave) and in terms of θ and r on the undisturbed surface of the fluid (see Figure 4). By carrying out the first integration in terms of x, one finds

$$V = \frac{\rho_F \mathrm{g}}{2} \int_0^a \int_0^{2\pi} \eta^2 r \, \mathrm{d}\theta \, \mathrm{d}r. \tag{66}$$

By substituting the potential function $\phi(x, r, \theta, t)$, given by equation (50), in the equation for the height of the fluid (32) and using equation (64), one obtains the matrix shape of η as

$$\eta = -\cos n\theta \{\mathbf{H}_\eta\}^{\mathrm{T}} [\mathbf{A}^{-1}] \{\mathbf{q}\}, \tag{67}$$

with

$$\{\mathbf{H}_\eta\}^{\mathrm{T}} = \left\{ \frac{\mathrm{J}_n(\mathrm{i}m_1 r)}{\mathrm{J}_n'(\mathrm{i}m_1 a)} \frac{\mathrm{J}_n(\mathrm{i}m_2 r)}{\mathrm{J}_n'(\mathrm{i}m_2 a)} \cdots \frac{\mathrm{J}_n(\mathrm{i}m_8 r)}{\mathrm{J}_n'(\mathrm{i}m_8 a)} \right\}^{\mathrm{T}}, \tag{68}$$

where $\boldsymbol{\lambda}_j$ are the roots of the characteristic equation (9), $\mathrm{i}^2 = -1$, a is the internal radius of the cylindrical shell and J_n is a Bessel function of the first kind of order n and J_n' is its derivative with respect to r.

One now substitutes the value of η given by equation (67) in the potential energy equation (66) to find its matrix form:

$$V = \frac{\pi \rho_F \mathrm{g}}{2} \{\mathbf{q}\}^{\mathrm{T}} [\mathbf{A}^{-1}]^{\mathrm{T}} \int_0^a \{\mathbf{H}_\eta\} \{\mathbf{H}_\eta\}^{\mathrm{T}} r \, \mathrm{d}r [\mathbf{A}^{-1}] \{\mathbf{q}\}. \tag{69}$$

The result of the integral in terms of r is

$$[\mathbf{hs}] = \int_0^a \{\mathbf{H}_\eta\} \{\mathbf{H}_\eta\}^{\mathrm{T}} r \, \mathrm{d}r. \tag{70}$$

Making use of equation (68), the general term of matrix [**hs**] is given and integrated in Appendix A.

The potential energy thus becomes

$$V = \tfrac{1}{2} \{\mathbf{q}\}^{\mathrm{T}} [\mathbf{k}_F] \{\mathbf{q}\}, \tag{71}$$

where

$$[\mathbf{k}_F] = \pi \rho_F \mathrm{g} [\mathbf{A}^{-1}]^{\mathrm{T}} [\mathbf{hs}] [\mathbf{A}^{-1}]. \tag{72}$$

The matrix $[\mathbf{k}_F]$ of equations (71) and (72) applies therefore only to the element which contains the free surface of the fluid and is due to the motion of this surface. The vertical displacement of the internal fluid does not contribute to the change in potential energy because it is continually replaced by the remaining fluid of the same density.

In general, the potential energy of any fluid element can be written as

$$V_e = \begin{cases} \frac{1}{2}\{\mathbf{q}\}^{\mathrm{T}}[\mathbf{k}_F]\{\mathbf{q}\}, & \text{for } e = 1 \text{ (element with free surface),} \\ \frac{1}{2}\{\mathbf{q}\}^{\mathrm{T}}[0]\{\mathbf{q}\} = 0, & \text{for } e > 1 \text{ (element without free surface).} \end{cases} \tag{73}$$

If one wishes to ignore the change in potential energy produced by the motion of the free surface, then $[\mathbf{k}_F]$ should be null. The matrix $[\mathbf{k}_F]$ developed in this study should not be confused with matrix $[\mathbf{k}_f]$ given in reference [11].

2.8. ANALYSIS OF THE FREE VIBRATIONS OF THE FLUID–SHELL SYSTEM

In section 2.3, the mass and stiffness matrices of the solid shell have been found to be symmetrical matrices with real, positive elements. Using these matrices, the kinetic and potential energies of the solid shell (in global co-ordinates) can be expressed as

$$T_0 = \tfrac{1}{2}\{\dot{\mathbf{\Delta}}\}^{\mathrm{T}}[\mathbf{M}_0]\{\dot{\mathbf{\Delta}}\}, \qquad V_0 = \tfrac{1}{2}\{\mathbf{\Delta}\}^{\mathrm{T}}[\mathbf{K}_0]\{\mathbf{\Delta}\}, \tag{74}$$

where $[\mathbf{M}_0]$ and $[\mathbf{K}_0]$ are given in reference [10].

To find the total energy of the system, one adds the kinetic and potential energies of the solid and fluid components:

$$T = T_0 + T_F = \tfrac{1}{2}\{\dot{\mathbf{\Delta}}\}^{\mathrm{T}}([\mathbf{M}_0] + [\mathbf{M}_F])\{\dot{\mathbf{\Delta}}\}, \qquad V = V_0 + V_F = \tfrac{1}{2}\{\mathbf{\Delta}\}^{\mathrm{T}}([\mathbf{K}_0] + [\mathbf{K}_F])\{\mathbf{\Delta}\}, \tag{75}$$

where $[\mathbf{M}_F]$ and $[\mathbf{K}_F]$ are the global matrices arising from $[\mathbf{m}_F]$ and $[\mathbf{k}_F]$, respectively.

Finally, the equations of motion are obtained by applying Lagrange's equations

$$\mathrm{d}/\mathrm{d}t\,[\partial T/\partial \dot{q}] + \partial V/\partial q = 0. \tag{76}$$

For solid and fluid cylinders, the following equation of motion which governs the dynamic behaviour of the fluid–shell system is obtained:

$$([\mathbf{M}_0] + [\mathbf{M}_F])\{\ddot{\mathbf{\Delta}}\} + ([\mathbf{K}_0] + [\mathbf{K}_F])\{\mathbf{\Delta}\} = \{0\}, \tag{77}$$

where $\{\mathbf{\Delta}\} = \{\boldsymbol{\delta}_1, \boldsymbol{\delta}_2, \ldots, \boldsymbol{\delta}_{N+1}\}^{\mathrm{T}}$.

In cases where the shell is not completely free, the kinematic boundary conditions must be taken into consideration. Thus, for a shell simply-supported at $x = 0$ and $x = L$, one must have $v_n = w_n = 0$ in the displacement vectors $\boldsymbol{\delta}_1$ and $\boldsymbol{\delta}_{N+1}$. To account for this, appropriate rows and columns of equation (A.20) are deleted, reducing the matrix equation to one of order $4(N + 1) - 4$ in the above example. In general, the order of the system will be $4(N + 1) - J$, where J is the number of kinematic boundary conditions imposed. The solution of equation (A.20) now follows by standard matrix techniques, yielding the natural frequencies, Ω_i, $i = 1, 2, \ldots, 4(N + 1) - J$, and the corresponding eigenvectors.

3. NUMERICAL CALCULATIONS AND DISCUSSION

Following the theory developed in the preceding sections, a computer program in FORTRAN language was created to calculate the natural frequencies of the system formed by the cylindrical shell and a fluid.

First, the cylindrical shell was divided into a sufficiently large number of finite elements to have good convergence. There are two principal steps in the calculation: the first corresponds to the calculations carried out to determine the natural frequencies of the solid shell, and the second takes into consideration the fluid–shell interaction.

The basic data entered into the program are: the number of finite elements, the number of circumferential modes, n, the mechanical properties of each section of the shell as a function of Young's modulus and Poisson's ratio, etc., the mass density of the shell, the

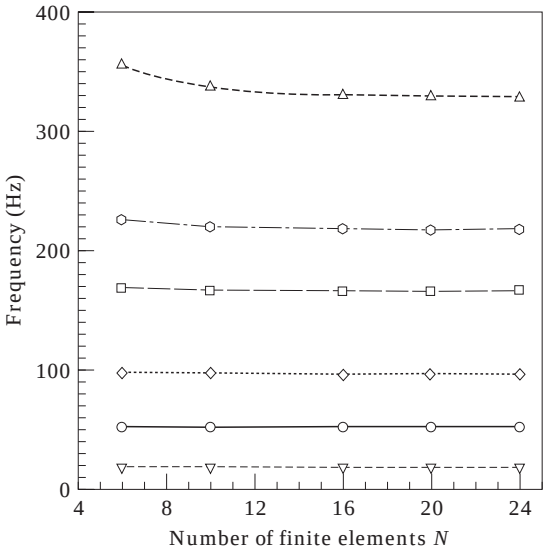

Figure 5. Analysis of convergence as a function of the number of finite elements for the clamped–free case, $n = 2$, $L/r = 5$, $r/t = 300$. m and H/L values respectively: —○—, 1, 0·5; —▽—, 1, 1·0; —□—, 2, 0·5; ····◇····, 2, 1·0; —△—, 3, 0·5; —⬡—, 3, 1·0.

geometry of the shell: average radius, thickness of the wall, length of the finite element, the boundary conditions, the density of the fluid, and the height of the fluid in the shell.

The principal steps in the calculation of the frequencies of the solid shell in interaction with the fluid are: the solution of the characteristic equation (9), the calculation of matrix $[\mathbf{A}]^{-1}$ and of all other intermediate matrices, the calculation of the elementary matrices $[\mathbf{m}_0]$ and $[\mathbf{k}_0]$, of an empty element, the calculation of the special Bessel functions, the calculation of the intermediate matrices, the calculation of the elementary matrices $[\mathbf{m}_F]$ and $[\mathbf{k}_F]$ in terms of the kinetic and potential energies, the assembly of the finite elements, the boundary conditions, and the solution to the problem in terms of eigenvalues and eigenvectors of the fluid–shell system.

3.1. ANALYSIS OF THE CONVERGENCE

The first numerical calculations were carried out to study the convergence of the solution as a function of the number of finite elements used to model the shell partially filled with fluid. For this purpose, a cylindrical shell with the following characteristics was used: length $L = 1{\cdot}524$ m, average radius $r = 0{\cdot}3048$ m, thickness of the wall $t = 1{\cdot}016$ mm, ratio $L/r = 5$, ratio $r/t = 300$, number of circumferential modes $n = 2$, boundary conditions: clamped–free.

The height of the fluid in the shell was considered for two cases: a cylindrical shell completely filled with fluid $H/L = 1{\cdot}00$, a cylindrical partially filled with fluid $H/L = 0{\cdot}50$.

The number of finite elements varied from six to twenty-four. For the axial mode the first seven frequencies were analysed. The results obtained are shown in Figure 5 and 6. The seventh frequency ($m = 7$), shows a maximum difference of 1·62% for $H/L = 0{\cdot}50$ and of 0·90% for $H/L = 1{\cdot}00$.

Figure 5 shows that, even with six elements, the values for the three first frequencies are stable. For the frequencies from four to seven, it can be seen in Figure 6 that stability is achieved when sixteen or more elements are used. One can therefore state that, for twenty elements, the values of the first seven frequencies converge towards the solution with a

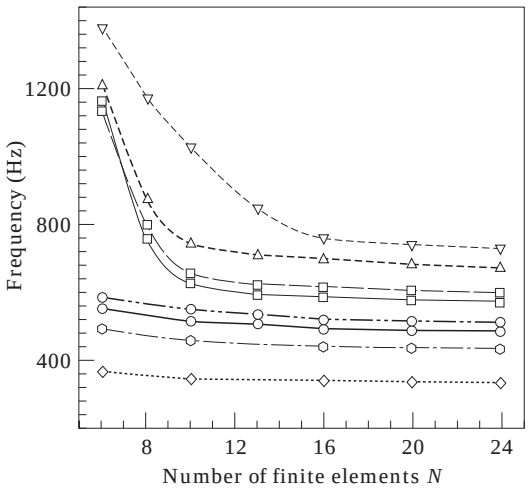

Figure 6. Analysis of convergence as a function of the number of finite elements for the clamped–free case, $n = 2$, $L/r = 5$, $r/t = 300$. m and H/L values respectively: —○—, 4, 0·5; ····◇····, 4, 1·0; —□—, m 5, 0·5; —⬡—, 5, 1·0; —△—, 6, 0·5; —○—, 6, 1·0; —▽—, 7, 0·5; —□—, 7, 1·0.

maximum deviation of 3%. Consequently, all subsequent calculations have been done using twenty elements.

3.2. VALIDATION OF THE MODEL

In order to analyse the theory developed in this work, a certain number of calculations have been made for different cases, to correspond to published experimental results.

The geometric dimensions given in reference [24] where three cylinders, A, B and C, are presented have been chosen and given the characteristics listed in Table 1.

The numerical results obtained by the methods outlined in this study and the theoretical and experimental results obtained in reference [24] are given in Table 2 and in Figure 7.

To the authors' great satisfaction, a maximum deviation of only 7% occurred between the present theory and the results given in reference [24] while the maximum deviation between the theory outlined in reference [24] and the experimental results in that work is of the order of 20%. This shows that there is good agreement between the theory developed in this work and the experimental results. An important factor in obtaining these results has been the use of specific displacement functions, drawn directly from thin shell theory.

TABLE 1

Data for three cylinders

	Cylinder A	Cylinder B	Cylinder C
Circumferential mode (n)	2, 3, 4	2, 3, 4	2, 3, 4
Axial mode (m)	1	1	1
Shell mass density (ρ_0 kg/dm^3)	7·75	7·75	7·75
Shell thickness (t mm)	0·65	0·82	1·16
Internal diameter (d_i mm)	198	198	198
Shell length (L mm)	280·1	325·5	398·0
Fluid height (%)	50	70	80
Boundary conditions	clamped–free	clamped–free	clamped–free
Fluid mass density (ρ_F kg/dm^3)	1·00	1·00	1·00

TABLE 2

Comparison between the theoretical results obtained with the present method on the one hand and the frequencies obtained experimentally in reference [24] *and the theoretical results of Reference* [24] *on the other hand. Cylinders A, B, C with the characteristic geometries given in Table* 1

Axial Mode $m = 1$			Frequencies (Hz)			Deviation in terms of exper. of Ref. [24] (%)	
Cyl.	H/L	n	Theory of ref. [24]	Present work	Exper. of ref. [24]	Theory of ref. [24]	Present work
A	0·5	2	544	495·0	490	11·02	1·02
		3	319	308·6	314	1·59	1·72
		4	275	277·8	276	0·36	0·65
B	0·7	2	350	312·3	298	17·45	4·80
		3	218	207·7	213	2·35	2·49
		4	229	240·1	247	7·29	2·79
C	0·8	2	244	218·7	203	20·20	7·73
		3	196	185·4	190	3·16	2·42
		4	251	290·2	296	15·20	1·96

These functions represent the real structural deformations well, and are more accurate than polynomial functions.

The theoretical model developed here shows a relatively small margin of error. One can therefore conclude that it fulfils the major purpose of this research: that of closely representing experimental reality.

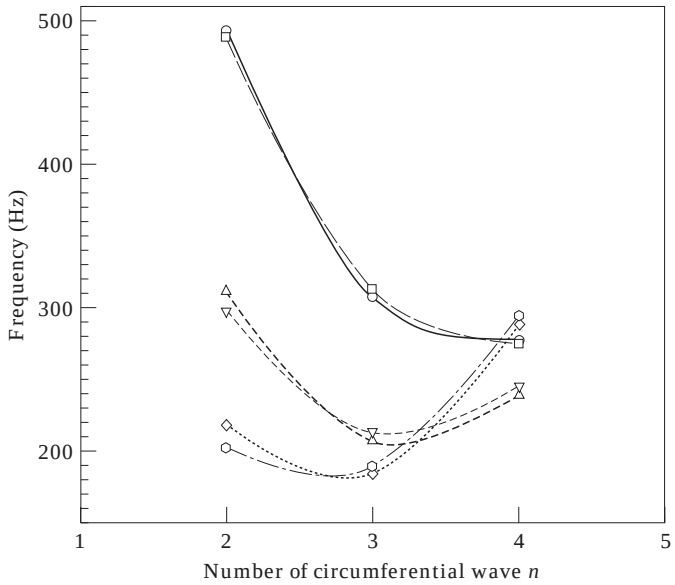

Figure 7. Validation of the theoretical model by a comparison of the numerical results of the present calculation method with the experimental results of reference [24]. For cylinder A: —○—, present study; —□—, experiment of reference [24]. For cylinder B: —△— present study; —▽—, experiment of reference [24]. For cylinder, ····◇····, present study; —⬡—, experiment of reference [24].

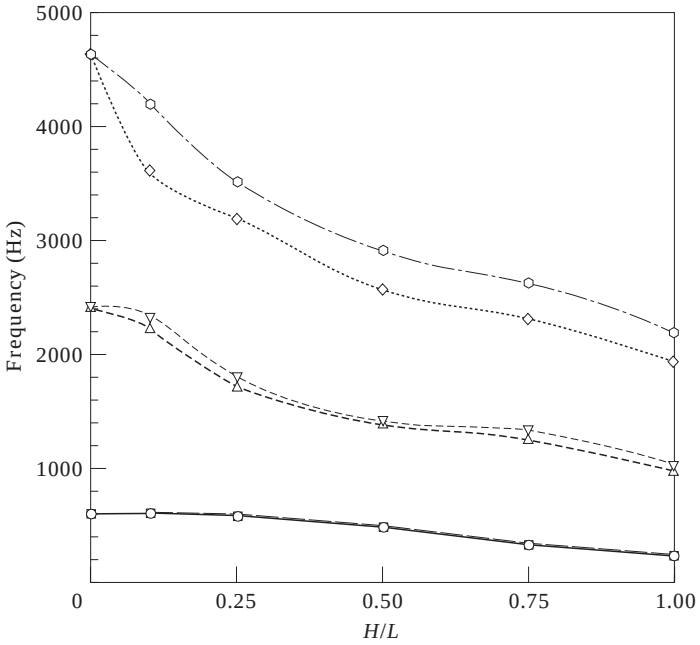

Figure 8. Comparison of theoretical frequencies between the results obtained with the present method (with surface effects) and those of reference [11] (without surface effects) for the clamped–free case, $n = 2$, $r/t = 100$, $L/r = 3$. For $m = 1$: —○—, present study; —□—, reference [11]. For $m = 2$: —△—, present study; —▽—, reference [11]. For $m = 3$: ····◇····, present study, —⬡—, reference [11].

3.3. THE INFLUENCE OF SURFACE MOTION

In order to determine the influence of motion of the free surface of the fluid, a comparative analysis is made of the numerical results obtained using the theory developed in the present study with that developed by Lakis *et al*. [11].

Several cylindrical shells are considered in order to provide a sufficiently large series of results to show the effect of the free surface during the vibrations. For a wall thickness $t = 1{\cdot}016$ mm, the geometric parameters of the shell are raised to include several characteristic values, as follows: the radius to thickness ratio ($r/t = 100, 300, 600, 900$), the length to radius ratio ($L/r = 3, 5, 7$), the level of the fluid in the shell ($H/L\%$; 25; 50; 100), axial modes analysed $m = 1, 2, \ldots, 7$, and circumferential modes analysed $n = 2, 3, \ldots, 13$.

In general, one notices that the frequencies calculated by the present method are lower than those given by Lakis *et al*. [11]. At the lower frequencies, the free surface effect is approximately 1–3%, which is negligible. In contrast, this effect becomes more pronounced, i.e., approximately 30%, in the case of the higher frequencies, $m = 7$ (see Figures 8 and 9 for $n = 2$; $m = 1$–7; $L/r = 3$; $r/t = 100$ and $H/L = 0{\cdot}00$–$1{\cdot}00$).

This phenomenon is attributed to the kinetic energy developed by the free surface in motion, which lowers the natural frequencies of the system to different levels as a function of other initial conditions: geometrical and physical characteristics, number of axial and circumferential modes.

The diameter of the shell also has a great influence on the vibrations of the fluid–shell system. The effect of the free surface is stronger particularly for wide shells, where one can see a reduction of the frequencies once there is a little fluid in the shell. The greatest

difference is observed at approximately $H/L = 0{\cdot}25$, whilst for fluid levels from $H/L = 0{\cdot}50$–$1{\cdot}00$ the variations are more moderate (see Figures 8 and 9).

Another factor is the length of the shell: in this case the tendency is the opposite of the preceding case, and one sees that the most significant deviations are to be found with the shortest shells, that is to say when $L/r = 3$. The higher the ratio L/r, the smaller the difference between the two methods. Similarly, one notes that whatever the ratio L/r may be, the smallest deviation between the frequencies occurs when the shell is full, $H/L = 1{\cdot}00$ (see Figure 10).

On the other hand, the potential energy due to the height of the waves has only a slight bearing on frequency variation, because it can readily be seen that it is far smaller than the strain energy of the solid shell. These conclusions are also based on a comparison of the values of the mass and stiffness matrices that have been developed during the numerical calculation process.

All these phenomena can be explained in terms of the theory developed in this work. In effect, the deviation between the frequencies predicted by the two methods is explained by the difference between the magnitudes of the kinetic energy developed on the free surface of the fluid and the kinetic energy developed on the lateral surface. The larger the free surface in comparison with the lateral surface surrounding the fluid, the greater its influence. This applies with a large r/t ratio, with small L/r ratios, and with low levels of fluid H/L.

Another influential parameter which was analysed is the number of circumferential modes (see Figures 11 to 13). For ratios $r/t = 300$, $L/r = 5$ and $H/L = 0{\cdot}50$, the number of circumferential modes was varied from 2 to 13. The notes that when the $n_{circumferential}$ is

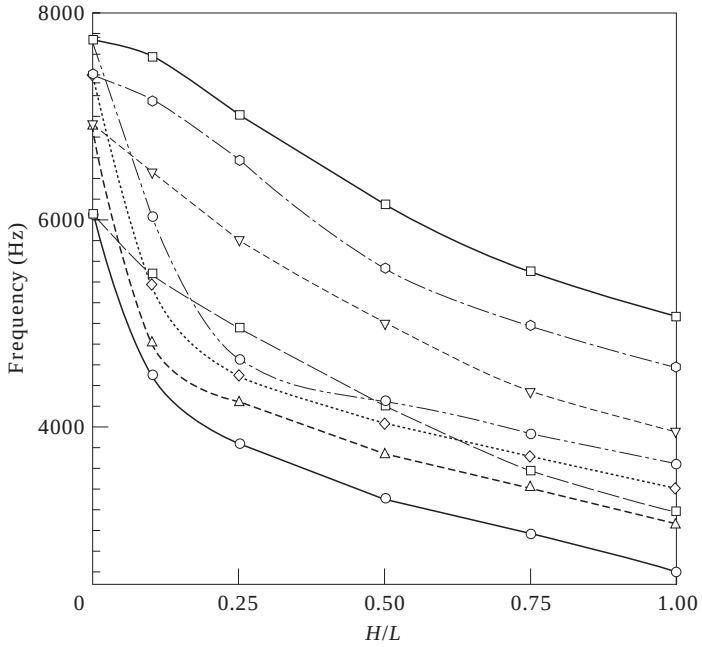

Figure 9. Comparison of theoretical frequencies between the results obtained with this method (with surface effects) and those of reference [11] (without surface effects) for the clamped–free case, $n = 2$, $r/t = 100$ and $L/r = 3$. For $m = 4$: —○—, present study; —□—, reference [11]. For $m = 5$: —△—, present study; —▽—, reference [11]. For $m = 6$; ····◇····, present study; —⬡—, reference [11]. For $m = 7$; —○—, present study; —□—; reference [11].

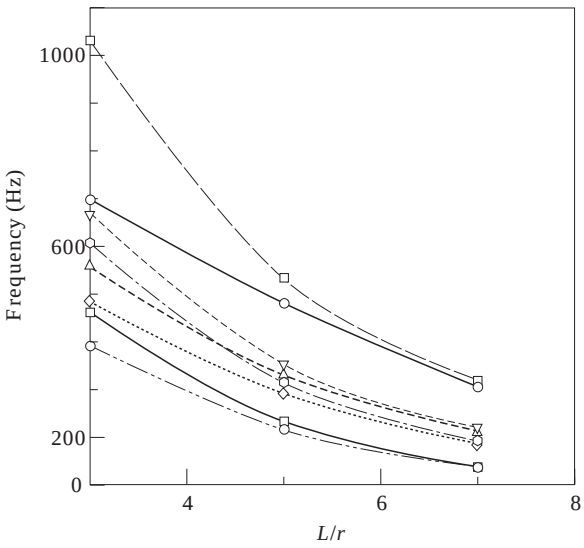

Figure 10. Frequency variation as a function of L/r and comparison between present study (with surface effects) with the results given in reference [11] (without surface effects) for $n = 2$, clamped–free case, $m = 3$ and $r/t = 300$. For $H/L = 0{\cdot}25$: —○—; present study, —□—; reference [11]. For $H/L = 0{\cdot}50$: —△—; present study, —▽—, reference [11]. For $H/L = 0{\cdot}75$; ····◇····, present study; —⬡—, reference [11]. For $H/L = 1{\cdot}00$: —○—, present study; —□—, reference [11].

increased, there is agreement between the two methods. Starting from a very low value, the deviation becomes slightly larger and stabilises at a maximum of 1% of difference. The surface effect is more marked for the lower values of the number of circumferential modes which correspond to the strain energy involved in stretching of the shell wall.

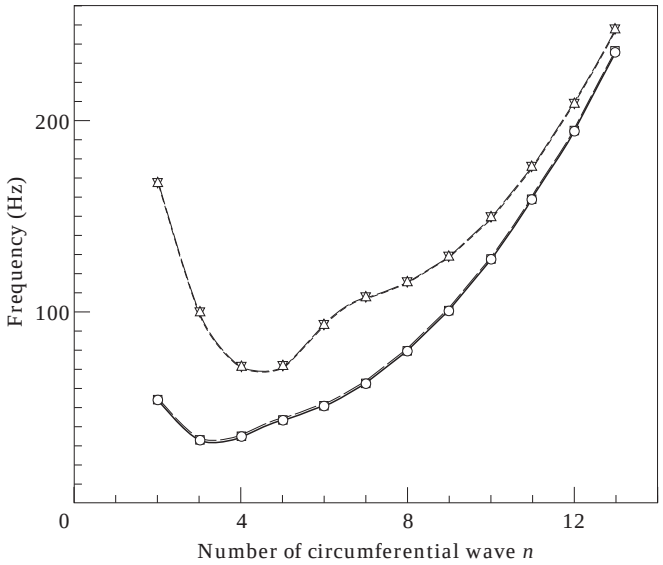

Figure 11. Frequency variation in terms of the circumferential mode and comparison with the results given in reference [11] (without surface effects) for $r/t = 300$, $L/r = 5$, $H/L = 0{\cdot}50$ and clamped–free case: For $m = 1$: —○—, present study; —□—, reference [11]. For $m = 2$: —△—, present study; —▽—, reference [11].

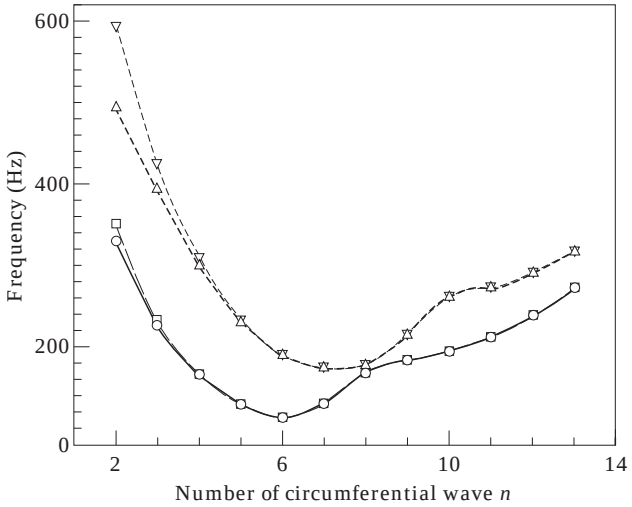

Figure 12. Frequency variation in terms of the circumferential mode and comparison with the results given in reference [11] (without surface effects) for $r/t = 300$, $L/r = 5$, $H/L = 0{\cdot}50$ and clamped–free case. For $m = 3$: —○—, present study; —□—, reference [11]. For $m=4$: —△—, present study; —▽—, reference [11].

The higher the number of circumferential modes, the more the strain energy of stretching decreases and the more the bending energy increases. In contrast, the free surface seems little influenced by bending strains at high frequencies and its effect is limited to no more than about 1% deviation.

The change in boundary conditions has the effect of increasing the frequencies proportionally to the other restrictions imposed. The variation in circumferential mode from two to thirteen was calculated for the case of a shell both simply supported and clamped–clamped and the results obtained are presented in Figures 14 and 15.

The deviation between the two methods follows the same pattern as in the case of the clamped–free shell, with the difference that the maximums found at $n = 2$ are slightly larger

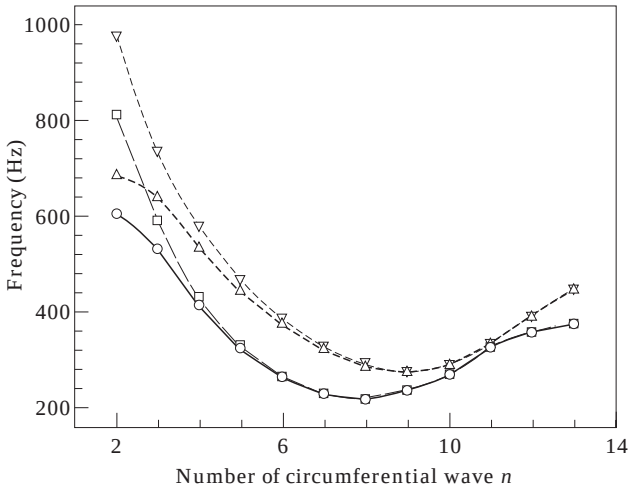

Figure 13. Frequency variation in terms of the circumferential mode and comparison with the results given in reference [11] (without surface effects) for $r/t = 300$, $L/r = 5$, $H/L = 0{\cdot}50$, clamped–free case. For $m = 5$: —○—, present study; —□—, reference [11]. For $m=6$ —△—, present study; —▽—, reference [11].

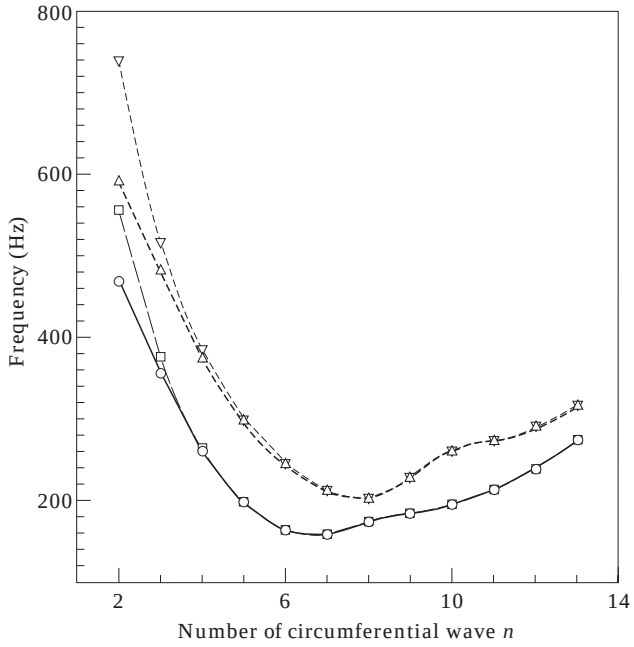

Figure 14. Frequency variation in terms of the circumferential mode and comparison with the results given in reference [11] (without surface effects) for $r/t = 300$; $L/r = 5$; $H/L = 0{\cdot}50$, simply supported–simply supported case. For $m = 3$: —○—, present study; —□—, reference [11]. For $m = 4$: —△—, present study; —▽—, reference [11].

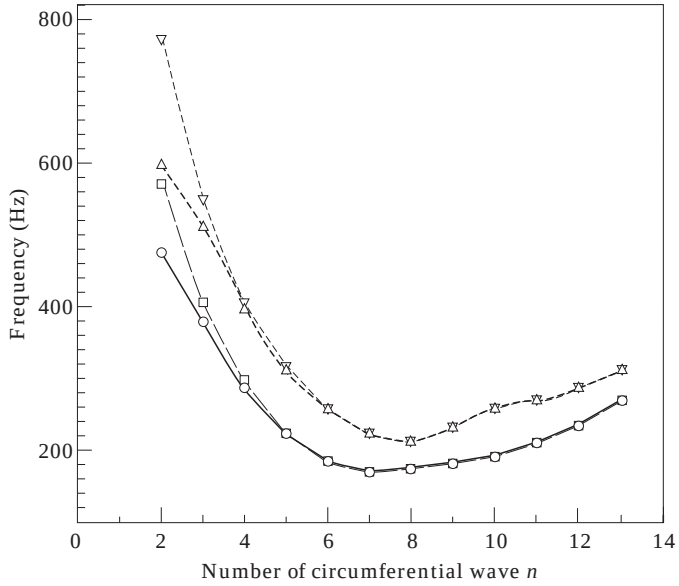

Figure 15. Frequency variation in terms of the circumferential mode and comparison with the results given in reference [11] (without surface effects) for $r/t = 300$, $L/r = 5$, $H/L = 0{\cdot}50$, clamped–clamped case. For $m = 3$: —○—, present study; —□—, reference [11]. For $m = 4$: —△—, present study; —▽—, reference [11].

than those for the first case. However, one notes that the slight increase is proportional to the number of restrictions imposed on the boundaries.

The deviation between the vectors which are predicted by the two methods follows the pattern which has been observed in the case of the frequencies. The differences are small for the first axial modes or when the ratio L/r is large (see Figures 16 and 17). However, these differences increase with the axial mode number (Figure 18) and with the ratio r/t.

Therefore, the effect of the free surface is more pronounced: (a) for wide shells ($r/t > 300$); (b) for shells having a low L/r ratio ($L/r < 5$), and (c) for low values of the number of circumferential modes n (predominant strain energy of the stretching wall). On the other hand, the free surface effect is considerably more pronounced (variation of 30%) for axial modes greater than 7 ($m > 7$). Finally the authors conclude that the natural frequencies of the empty shells in the mode under consideration are high compared with the natural frequencies of the free surface phenomena, at least in the lowest modes ($m \leqslant 7$); accordingly, coupling between the shell modes and the liquid free surface modes is weak. On the other hand, Lindholm *et al*. [1] have found experimentally that there is a possibility of non-linear coupling between the low frequency, free surface modes, resulting in subharmonic excitation of the former while the shell itself is oscillating at high frequencies.

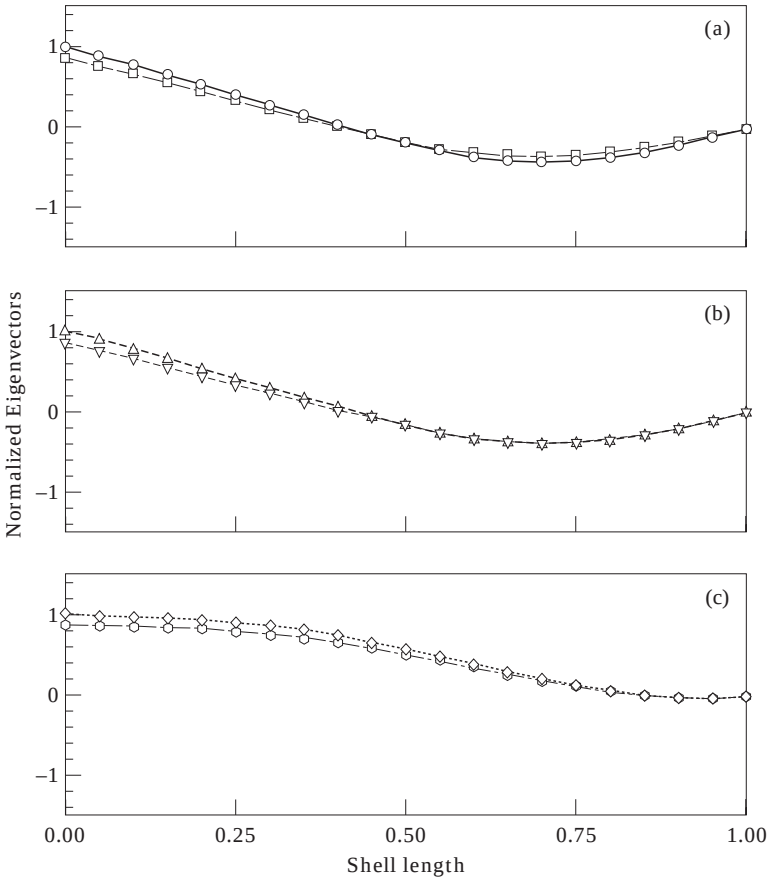

Figure 16. Comparison between the normalised eigenvectors of the present method (with surface effects) and those of Reference [11] (without surface effects) for $n = 2$; $m = 2$; $r/t = 100$; $L/r = 3$; $H/L = 0{\cdot}50$, clamped–free; where (a) V/V_{max}: —○—, present study, —□—, reference [11]; (b) W/W_{max}: —△—, present study; —▽— , reference [11]; (c) U/U_{max} ····◇····, present study; —⬡—, reference [11].

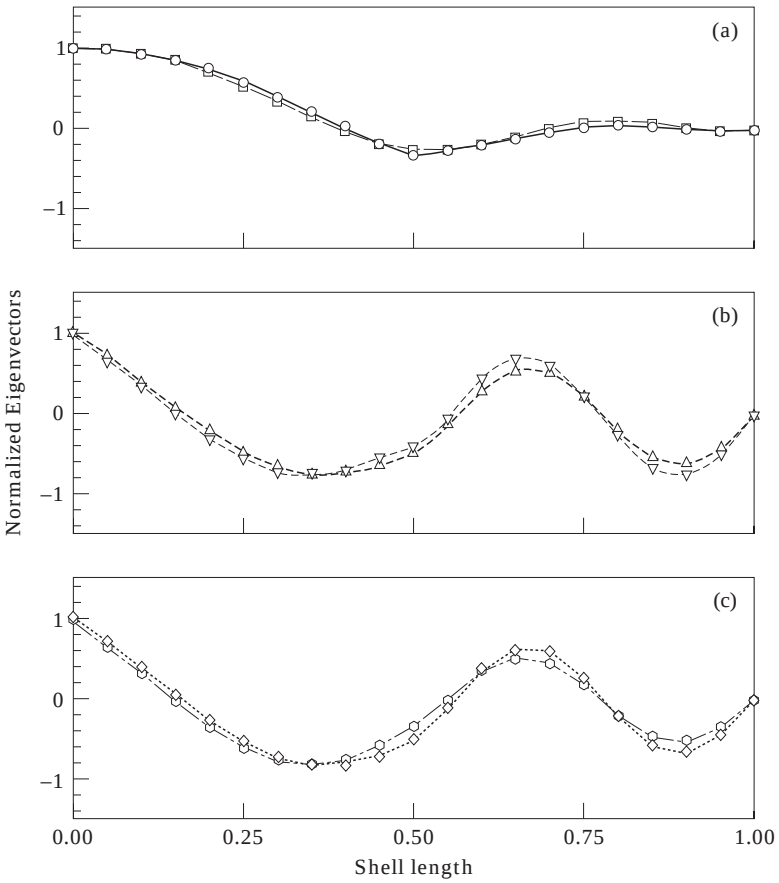

Figure 17. Comparison between the normalised eigenvectors of the present method (with surface effects) and those of reference [11] (without surface effects) for $n = 2$, $m = 4$, $r/t = 100$, $L/r = 3$, $H/L = 0{\cdot}50$, clamped–free; where (a) U/U_{max}: —○—, present study; —□—, reference [11]; (b) V/V_{max} —△—, present study; —▽—, reference [11]; (c) W/W_{max} ····◇····, present study; —⬡—, reference [11].

The next step for the authors' research is to investigate the non-linear effects of the free surface.

4. CONCLUSION

The authors present, in this paper, a new method for the dynamic analysis of thin cylindrical shells which takes into consideration the effects of the free surface of the fluid. It is particularly significant that this method uses displacement functions derived from classical thin shell theory and incorporates them into the finite element method. This has clear advantages. Since the specific displacement functions model the displacements of the structures better, the number of finite elements is reduced, which decreases the necessary calculation time.

The influence of the free surface is evaluated by considering the kinetic and potential energies which are present during vibrational motion. The numerical results calculated using a computer program show good agreement with the experimental results of reference [24]. The potential function found using the condition of permeability at the wall satisfactorily models the behaviour of the fluid and of the free surface during the shell's

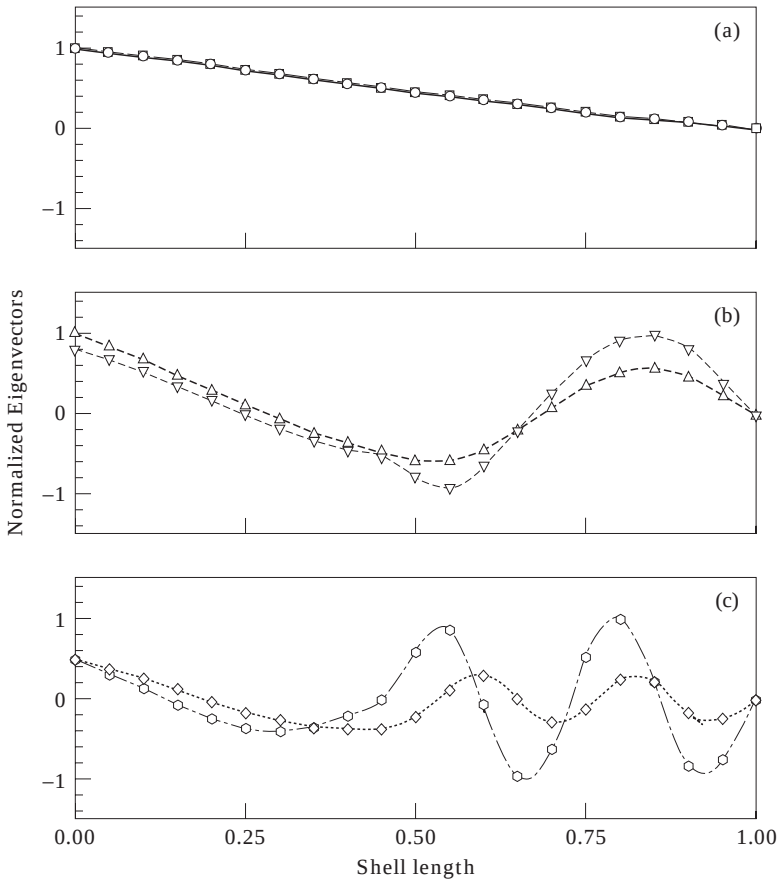

Figure 18. Comparison between the normalised eigevectors of this method (with surface effects) and those of reference [11] (without surface effects) for $n = 2$, $m = 6$, $r/t = 100$, $L/r = 3$, $H/L = 0{\cdot}50$, clamped–free; where (a) U/U_{max}: —○—, present study; —□—, reference [11]; (b) V/V_{max}: —△—, present study; —▽—, reference [11], (c) W/W_{mx} ····◇····, present study; —⬡—, reference [11].

vibration. This model can therefore satisfactorily predict the vibration characteristics of orthotropic cylindrical shells partially filled with fluid.

The authors have carried out a comparative analysis of the influence of surface motion for different geometries and different levels of fluid in cylindrical shells, in order to establish the parameters which determine the strongest free surface oscillations. As this work is part of a larger study on the dynamics of thin shells, the next logical step will be the assembly of the spherical, cylindrical and conical elements developed thus far in order to produce a geometry applicable to any shell of revolution.

REFERENCES

1. U. S. Lindholm, D. D. Kana and H. N. Abramson 1962 *Journal of the Aerospace Sciences* **29**, 1052–1059. Breathing vibrations of a circular cylindrical shell with an internal liquid.
2. F. I. Niordson 1953 *Kungliga Tekniska högskolans handlingar* No. 73. Vibrations of a cylindrical tube containing flowing fluid.
3. R. W. Gregory and M. P. Paidoussis 1966 *Proceedings of the Royal Society* A **293**, 512–527. Unstable oscillation of tubular cantilevers conveying fluid. I. Theory.

4. M. P. Paidoussis and J.-P. Denise 1971 *Journal of Sound and Vibration* **16**, 459–461. Flutter of cylindrical shells conveying fluid.
5. H. Lamb 1945 *Hydrodynamics*. New York: Dover Publications, sixth edition.
6. J. G. Berry and E. Reissner 1958 *Journal of Aerospace Science* **25**, 288–294. The effect of an internal compressible fluid column on the breathing vibrations of a thin pressurized cylindrical shell.
7. C. W. Coale and M. Nagano 1965 *AIAA Symposium on Structural Dynamics and Aeroelasticity*. Axisymmetric modes of an elastic cylindrical–hemispherical tank partially filled with liquid.
8. A. A. Lakis, P. Van Dyke and H. Ouriche 1992 *Journal of Fluid and Structures* **6**, 135–162. Dynamic analysis of anisotropic fluid-filled conical shells.
9. A. A. Lakis 1976 *Second Intelligence Symposium on Finite Element Methods in Flow Problems*, *International Congress for C.A.D.*, *Santa Margherita Ligure*, *Italy*, *June* 14–18; **76**, 263–271. Theoretical model of cylindrical structures containing turbulent flowing fluids.
10. A. A. Lakis and M. P. Paidoussis 1972 *Journal of Mechanical Science* **14**, 49–71. Dynamic analysis of axially non-uniform thin cylindrical shells.
11. A. A. Lakis and M. P. Paidoussis 1971 *Journal of Sound and Vibration* **19**, 1–15. Free vibration of cylindrical shells partially filled with liquid.
12. A. A. Lakis and M. P. Paidoussis 1972 *Journal of Sound and Vibration* **25**, 1–27. Prediction of the response of a cylindrical shell to arbitrary or boundary layer induced random pressure fields.
13. H. F. Bauer 1995 *Journal of Sound and Vibration* **180**, 689–704. Coupled frequencies of a liquid in a circular cylindrical container with elastic liquid surface cover.
14. N. Yamaki, J. Tani and T. Yamaji 1984 *Journal of Sound and Vibration* **94**, 531–550. Free vibration of a clamped–clamped circular cylindrical shell partially filled with an internal liquid.
15. T. Mazúch, J. Horáček, J. Trnka and J. Veselý 1996 *Journal of Sound and Vibration* **193**, 669–690 Natural modes of a thin clamped–free steel cylindrical storage tank partially filled with water: FEM and measurement.
16. P. B. Gonçalves and N. R. S. S. Ramos 1996 *Journal of Sound and Vibration* **195**, 429–444. Free vibration analysis of cylindrical tanks partially filled with liquid.
17. A. A. Lakis and M. Sinno 1992 *International Journal for Numerical Methods in Engineering* **33**, 235–268. Free vibration of axisymmetric and beam-like cylindrical shells, partially filled with liquid.
18. J. L. Sanders 1959 *NASA TR-R*24. An improved first approximation theory for thin shells.
19. B. Budiansky and J. L. Sanders 1963 *Progress in Applied Mechanics*, The Prager Anniversary Volume 129–140. On the "best" first order linear shell theory.
20. A. A. Lakis and M. P. Paidoussis 1970 *Mechanical Engineering Research Laboratories Report* 70-9, *McGill University*. Dynamic analysis of axially non-uniform, thin cylindrical shells. I. Matrix formulation.
21. J. L. Sanders 1959 *NASA TR-R*24. An improved first approximation theory for thin shells.
22. A. A. Lakis and A. Laveau 1991 *International Journal of Solids and Structures* **28**, 1079–1094. Non-linear dynamic analysis of anisotropic shells containing a flowing fluid.
23. A. A. Lakis 1971 *Ph.D. Thesis*, *McGill University*. Free vibration and response to random pressure field of non-uniform shells.
24. J. Mistry and J. C. Menezes 1995 *Journal of Vibration and Acoustics* **117**, 87–93. Vibration of cylinders partially filled with liquid.
25. G. N. Watson 1958 *A Treatise On The Theory of Bessel Functions*. Cambridge, University Press.

APPENDIX A: EQUATIONS

A.1. KINEMATIC EQUATIONS

$$\epsilon_x = \partial U/\partial x, \qquad k_x = -\partial^2 W/\partial x^2, \qquad \epsilon_\theta = (1/r)\,\partial V/\partial\theta + W/r,$$

$$k_\theta = -(1/r^2)\,\partial^2 W/\partial\theta^2 + (1/r^2)\,\partial V/\partial\theta, \qquad \epsilon_{x\theta} = \tfrac{1}{2}(\partial V/\partial x + (1/r)\,\partial U/\partial\theta),$$

$$k_{x\theta} = -(1/r)\,\partial^2 W/\partial x\,\partial\theta + (3/4r)\,\partial V/\partial x - (1/4r^2)\,\partial U/\partial\theta. \tag{A.1}$$

A.2. STRESS–STRAIN EQUATIONS

$$N_x = D(\epsilon_x + v\epsilon_\theta), \qquad M_x = K(k_x + vk_\theta), \qquad N_\theta = D(\epsilon_\theta + v\epsilon_x), \qquad M_\theta = K(k_\theta + vk_x),$$
$$N_{x\theta} = D(1-v)\epsilon_{x\theta}, \qquad M_{x\theta} = K(1-v)k_{x\theta}. \tag{A.2}$$

Stiffness parameters:

$$K = Et^3/12(1-v^2), \qquad D = Et/(1-v)^2. \tag{A.3}$$

A.3. SANDERS' EQUILIBRIUM EQUATIONS IN TERMS OF DISPLACEMENTS U, V AND W

$$r^2\frac{\partial^2 U}{\partial x^2} + \frac{(1-v)}{2}\frac{\partial^2 U}{\partial \theta^2} + \frac{r(1+v)}{2}\frac{\partial^2 V}{\partial x\,\partial\theta} + rv\frac{\partial W}{\partial x}$$
$$+ k\left[\frac{(1-v)}{8}\frac{\partial^2 U}{\partial\theta^2} - \frac{3(1-v)r}{8}\frac{\partial^2 V}{\partial x\,\partial\theta} + \frac{(1-v)r}{2}\frac{\partial^3 W}{\partial x\,\partial\theta^2}\right] = 0, \tag{A.4}$$

$$\frac{(1+v)r}{2}\frac{\partial^2 U}{\partial x\,\partial\theta} + \frac{\partial^2 V}{\partial\theta^2} + \frac{(1-v)r^2}{2}\frac{\partial^2 V}{\partial x^2} + \frac{\partial W}{\partial\theta}$$
$$+ k\left[-\frac{3(1-v)r}{8}\frac{\partial^2 U}{\partial x\,\partial\theta} + \frac{9(1-v)r^2}{8}\frac{\partial^2 V}{\partial x^2} + \frac{\partial^2 V}{\partial\theta^2} - \frac{(3-v)r^2}{2}\frac{\partial^2 W}{\partial x^2\,\partial\theta} - \frac{\partial^3 W}{\partial\theta^3}\right] = 0, \tag{A.5}$$

$$-vr\frac{\partial U}{\partial x} - \frac{\partial V}{\partial\theta} - W + k\left[\frac{(v-1)r}{2}\frac{\partial^3 U}{\partial x\,\partial\theta^2} + \frac{(3-v)r^2}{2}\frac{\partial^3 V}{\partial x^2\,\partial\theta} + \frac{\partial^3 V}{\partial\theta^3} - r^4\frac{\partial^4 W}{\partial x^4}\right.$$
$$\left. - 2r^2\frac{\partial^4 W}{\partial x^2\,\partial\theta^2} - \frac{\partial^4 W}{\partial\theta^4}\right] = 0, \tag{A.6}$$

where $k = (1/12)(t/r)^2$.

A.4. CHARACTERISTIC EQUATION

Matrix [**H**] is

$$[\mathbf{H}] = \begin{Bmatrix} A_j \\ B_j \\ C_j \end{Bmatrix} = \begin{bmatrix} H_{11} & H_{12} & H_{13} \\ H_{21} & H_{22} & H_{23} \\ H_{31} & H_{32} & H_{33} \end{bmatrix} \begin{Bmatrix} A_j \\ B_j \\ C_j \end{Bmatrix}, \quad \text{with } j = 1, 2, \ldots, 8. \tag{A.7}$$

By expressing A_j and B_j in terms of C_j:

$$A_i = \alpha_j C_j, \qquad B_j = \beta_j C_j, \tag{A.8}$$

One obtains

$$\begin{bmatrix} H_{11} & H_{12} \\ H_{21} & H_{22} \end{bmatrix} \begin{Bmatrix} \alpha_j \\ \beta_j \end{Bmatrix} = \begin{Bmatrix} -H_{13} \\ -H_{23} \end{Bmatrix}, \quad \text{with } j = 1, 2, \ldots, 8. \tag{A.9}$$

The coefficients required to solve system (A.9) are

$$H_{11} = \boldsymbol{\lambda}_j^2 - (1 - \nu/2)n^2(1 + k/4), \qquad H_{12} = (n\boldsymbol{\lambda}_j/2)\left[\nu(1 + \tfrac{3}{4}k) + (1 - \tfrac{3}{4}k\right)\Big)\Big],$$

$$H_{21} = H_{12}, \qquad H_{22} = -(1 - \nu/2)\boldsymbol{\lambda}_j^2 + n^2(1 + k) - \tfrac{9}{8}(1 - \nu)\, k\boldsymbol{\lambda}_j^2,$$

$$H_{13} = \nu\boldsymbol{\lambda}_j - (1 - \nu/2)k\boldsymbol{\lambda}_j n^2, \qquad H_{23} = n(1 + n^2 k) - (3 - \nu/2)kn\boldsymbol{\lambda}_j^2, \tag{A.10}$$

with the provision that

$$H_{11}H_{22} - H_{21}H_{12} = -(1 - \nu/2)(\boldsymbol{\lambda}^2 - n^2)^2 \neq 0. \tag{A.11}$$

A.5. MATRIX [A] (8,8)

$$\begin{Bmatrix} \boldsymbol{\delta}_i \\ \boldsymbol{\delta}_j \end{Bmatrix} = [\mathbf{A}]\{\mathbf{C}\}. \tag{A.12}$$

The terms for each line of matrix [**A**] are given by (for $i = 1, \ldots, 8$)

$$A(1, i) = \alpha_i, \qquad A(2, i) = 1, \qquad A(3, i) = \boldsymbol{\lambda}_i/r, \qquad A(4, i) = \beta_i,$$

$$A(5, i) = \alpha_i\, \mathrm{e}^{\boldsymbol{\lambda}_i 1/r}, \qquad A(6, i) = \mathrm{e}^{\boldsymbol{\lambda}_i 1/r}, \qquad A(7, i) = \frac{\boldsymbol{\lambda}_i}{r}\, \mathrm{e}^{\boldsymbol{\lambda}_i 1/r}, \qquad A(8, i) = \beta_i\, \mathrm{e}^{\boldsymbol{\lambda}_i 1/r}. \tag{A.13}$$

A.6. MATRIX [R] (3, 8)

The terms for each line of matrix [**R**] are given by ($i = 1, \ldots, 8$)

$$R(1, i) = \alpha_i\, \mathrm{e}^{\boldsymbol{\lambda}_i x/r}, \qquad R(2, i) = \mathrm{e}^{\boldsymbol{\lambda}_i x/r}, \qquad R(3, i) = \beta_i\, \mathrm{e}^{\boldsymbol{\lambda}_i x/r}. \tag{A.14}$$

A.7. MATRIX [T] (3, 3)

$$[\mathbf{T}] = \begin{bmatrix} \cos(n\theta) & 0 & 0 \\ 0 & \cos(n\theta) & 0 \\ 0 & 0 & \sin(n\theta) \end{bmatrix}. \tag{A.15}$$

A.8. MATRIX [Q] (6, 8)

For $i = 1, \ldots, 8$, the terms for each line of matrix [**Q**] are given by

$$Q(1, i) = \alpha_i(\boldsymbol{\lambda}_i/r)\, \mathrm{e}^{\boldsymbol{\lambda}_i x/r}, \qquad Q(2, i) = (1/r)(n\beta_i + 1)\, \mathrm{e}^{\boldsymbol{\lambda}_i x/r},$$

$$Q(3, i) = (1/r)(\beta_i\boldsymbol{\lambda}_i - n\alpha_i)\, \mathrm{e}^{\boldsymbol{\lambda}_i x/r}, \qquad Q(4, i) = -(\boldsymbol{\lambda}_i/r)^2\, \mathrm{e}^{\boldsymbol{\lambda}_i x/r},$$

$$Q(5, i) = (1/r^2)(n^2 + \beta_i n)\, \mathrm{e}^{\boldsymbol{\lambda}_i x/r}, \qquad Q(6, i) = (1/r^2)(2n\boldsymbol{\lambda}_i + \tfrac{3}{2}\beta_i\boldsymbol{\lambda}_i + \tfrac{1}{2}n\alpha_i)\, \mathrm{e}^{\boldsymbol{\lambda}_i x/r}. \tag{A.16}$$

A.9. CALCULATION OF THE SUMMATION OF THE FLUID MASS MATRICES

The total kinetic energy of a fluid finite element is given by equations (62) where the summation of the mass matrices can be written as

$$[\mathbf{m}_f] = [\mathbf{m}_x] + [\mathbf{m}_r] + [\mathbf{m}_\theta]. \tag{A.17}$$

Using equations (57), (58) and (61) one can write

$$[\mathbf{m}_f] = \pi\rho[\mathbf{A}^{-1}]^{\mathrm{T}}([\mathbf{hx}] + [\mathbf{hr}] + [\mathbf{h\theta}])[\mathbf{A}^{-1}]. \tag{A.18}$$

Therefore, the general term $[\mathbf{hx}] + [\mathbf{hr}] + [\mathbf{h\theta}]$ can be written as

$$h_{jk} = hx_{jk} + hr_{jk} + h\theta_{jk}, \tag{A.19}$$

where (1) for $\mathrm{i}m_j \neq \mathrm{i}m_k$:

$$h_{jk} = \frac{ar_{jk}}{\mathrm{J}'_n(i\boldsymbol{\lambda}_j)\mathrm{J}'_n(\mathrm{i}\boldsymbol{\lambda}_k)}\left[\frac{\mathrm{i}\mathbf{m}_j \mathrm{J}_{n+1}(\mathrm{i}m_j a)\mathrm{J}_n(\mathrm{i}m_k a) - \mathrm{i}m_k \mathrm{J}_n(\mathrm{i}m_j a)\mathrm{J}_{n+1}(\mathrm{i}m_k a)}{(\mathrm{i}m_j)^2 - (\mathrm{i}m_k)^2}\right.$$

$$+ \mathrm{i}m_j \mathrm{J}_n(\mathrm{i}m_j a)\mathrm{J}_{n-1}(\mathrm{i}m_k a) - \mathrm{i}m_k \mathrm{J}_{n-1}(\mathrm{i}m_j a)\mathrm{J}_n(\mathrm{i}m_k a)/2(\mathrm{i}m_j)^2 - (\mathrm{i}m_k)^2$$

$$\left. + \mathrm{i}m_j \mathrm{J}_{n+2}(\mathrm{i}m_j a)\mathrm{J}_{n+1}(\mathrm{i}m_k a) - \mathrm{i}m_k \mathrm{J}_{n+1}(\mathrm{i}m_j a)\mathrm{J}_{n+2}(\mathrm{i}m_k a)/2(\mathrm{i}m_j)^2 - (\mathrm{i}m_k)^2\right], \tag{A.20}$$

(2) for $\mathrm{i}m_j = \mathrm{i}m_k$:

$$h_{jk} = \frac{r_{jk}}{\mathrm{J}'_n(\mathrm{i}\boldsymbol{\lambda}_j)\mathrm{J}'_n(\mathrm{i}\boldsymbol{\lambda}_k)}\frac{a^2}{2}[\mathrm{J}_n^2(\mathrm{i}m_k a) - \mathrm{J}_{n-1}(\mathrm{i}m_k a)\mathrm{J}_{n+1}(\mathrm{i}m_k a)$$

$$+ [(\mathrm{J}_{n-1}^2(\mathrm{i}m_k a) - \mathrm{J}_{n-2}(\mathrm{i}m_k a)\mathrm{J}_n(\mathrm{i}m_k a)]/2 + [\mathrm{J}_{n+1}^2(\mathrm{i}m_k a) - \mathrm{J}_n(\mathrm{i}m_k a)\mathrm{J}_{n+2}(\mathrm{i}m_k a)]/2]. \tag{A.21}$$

A.10. CALCULATION OF THE FLUID STIFFNESS MATRIX

One wants to calculate the fluid stiffness matrix (72) where the [**hs**] terms can be taken from equations (68) and (70) as follows:

$$hs_{jk} = \frac{1}{\mathrm{J}'_n(\mathrm{i}\boldsymbol{\lambda}_j)\mathrm{J}'_n(\mathrm{i}\boldsymbol{\lambda}_k)}\int_0^a r\mathrm{J}_n(\mathrm{i}m_j r)\mathrm{J}_n(\mathrm{i}m_k r)\,\mathrm{d}r, \qquad \text{with } j, k = 1, 2, \ldots, 8. \tag{A.22}$$

This integral is calculated using Lommel's formulae (see Watson [25]). Therefore:

(1) for $\mathrm{i}m_j \neq \mathrm{i}m_k$:

$$hs_{jk} = \frac{ar_{jk}}{\mathrm{J}'_n(\mathrm{i}\boldsymbol{\lambda}_j)\mathbf{J}'_n(\mathrm{i}\boldsymbol{\lambda}_k)}\frac{\mathrm{i}m_j \mathrm{J}_{n+1}(\mathrm{i}m_j a)\mathrm{J}_n(\mathrm{i}m_k a) - \mathrm{i}m_k \mathrm{J}_n(\mathrm{i}m_j a)\mathrm{J}_{n+1}(\mathrm{i}m_k a)}{(\mathrm{i}m_j)^2 - (\mathrm{i}m_k)^2}, \tag{A.23}$$

(2) for $\mathrm{i}m_j = \mathrm{i}m_k$:

$$hs_{jk} = \frac{r_{jk}}{\mathrm{J}'_n(\mathrm{i}\boldsymbol{\lambda}_j)\mathrm{J}'_n(\mathrm{i}\boldsymbol{\lambda}_k)}\frac{a^2}{2}[\mathrm{J}_n^2(\mathrm{i}m_k a) - \mathrm{J}_{n-1}(\mathrm{i}m_k a)\mathrm{J}_{n+1}(\mathrm{i}m_k a)], \tag{A.24}$$

where $\mathrm{i}m_j = \mathrm{i}\boldsymbol{\lambda}_j/a$, $\mathrm{i}^2 = -1$, a is the internal radius of the cylindrical shell, $\mathrm{J}_n(\mathrm{i}m_j a)$ is a Bessel function of the first type of order n and $\mathrm{J}'_n(\mathrm{i}\boldsymbol{\lambda}_j)$ is the derivative of $\mathrm{J}_n(\mathrm{i}m_j r)$ with respect to r.

APPENDIX B: LIST OF SYMBOLS

a	internal radius of the shell	$\{\mathbf{C}\}$	vector of the arbitrary constants defined by equation (11)
A_1, A_2	Lamé's parameters		
A_j, B_j, C_j	constants defined by equations (7) and (8)	D	membrane stiffness
		E	Young's modulus

$\{\mathbf{F}\}^e$	external force vector
$\{\mathbf{F}_j\}_k$, $\{\mathbf{F}_i\}_{k+1}$	internal force vector at node j of element k and at node i of element $(k+1)$
g	acceleration of gravity
H	height of fluid in the shell
$\{\mathbf{H}_\eta\}$	vector defined by equation (68)
$\mathbf{J}_n$	Bessel function of the first kind and of order n
k_i	virtual parts of λ_i
K	bending stiffness
l	length of a finite element
L	length of the shell
M_1, M_2, $\bar{M}_{12}$	resultant bending stresses
M_x, M_θ, $\bar{M}_{x\theta}$	resultant bending stresses in cylindrical co-ordinates
N	number of finite elements
N_1, N_2, $\bar{N}_{12}$	resultant membrane stresses
N_x, N_θ, $\bar{N}_{x\theta}$	resultant membrane stresses in cylindrical co-ordinates
n	number of circumferential modes
Q_1, Q_2	resultant shear stresses
Q_x, Q_θ	resultant shear stresses in cylindrical co-ordinates
$\{\mathbf{q}\} = \begin{Bmatrix}\boldsymbol{\delta}_i \\ \boldsymbol{\delta}_j\end{Bmatrix}$	displacement vector, in local co-ordinates, at nodes i and j of the finite element
$\{\mathbf{q}\}_e$	displacement vector of element e
r	average shell radius in equations (1–24); r also indicates the radial direction of the cylinder in equations (26–72)
R_1, R_2	radii of curvature of the mean surface
$\{\mathbf{R}_F\}$	matrix defined by equation (49)
t	thickness of the shell wall; t also indicates "time" in the continuity equation
U	axial displacement
V	circumferential displacement
W	radial displacement
x	axial co-ordinate
Y_n	Bessel function of the second kind and of order n
α_i, β_i	defined by equation (10)
$\boldsymbol{\delta}_i$, $\boldsymbol{\delta}_j$	ensemble of the four displacements of each node, defined by equations (13) and (14)
$\{\boldsymbol{\delta}\}$	displacement vector in global co-ordinates
$\{\boldsymbol{\epsilon}\}$	deformation vector defined by equation (17)
$\{\boldsymbol{\sigma}\}$	stress vector defined by equation (18)
ϕ	function of velocity potential
μ_i	imaginary parts of $\boldsymbol{\lambda}_i$
η	height of the wave
ξ_i, ξ_2	co-ordinates of the mean surface
θ	circumferential co-ordinate
ω	natural frequency
ν	Poisson's ratio
ρ	density of the shell
ρ_F	density of the fluid

MATRICES

[A]	matrix defined by equation (14)
[B]	matrix defined by equation (17)
[H]	matrix defined by equation (8)
$[\mathbf{H}_F]$	matrix defined by equation (52)
$[\mathbf{H}_x]$	matrix defined by equation (55)
[hr]	matrix defined by equation (A.18)
[hs]	matrix defined by equation (70)
[hx]	matrix defined by equation (A.18)
[hθ]	matrix defined by equation (A.18)
$[\mathbf{k}_0]$	matrix defined by equation (22)
$[\mathbf{k}_F]$	matrix defined by equation (72)
$[\mathbf{K}_0]$	stiffness matrix for the whole shell
$[\mathbf{K}_F]$	stiffness matrix for the whole fluid
$[\mathbf{m}_0]$	matrix defined by equation (23)
$[\mathbf{m}_F]$	matrix defined by equation (62)
$[\mathbf{m}_R]$	matrix defined by equation (59)
$[\mathbf{m}_x]$	matrix defined by equation (59)
$[\mathbf{m}_\theta]$	matrix defined by equation (61)
$[\mathbf{M}_0]$	mass matrix for the whole shell
$[\mathbf{M}_F]$	mass matrix for the whole fluid
[N]	matrix defined by equation (16)
[P]	matrix defined by equation (19)
[Q]	matrix defined by equation (17)
[R]	matrix defined by equation (11)
[T]	matrix defined by equation (11)